Title: A florigen paralog is required for short-day vernalization in a pooid grass.

Authors: Daniel P. Woods [1,2,3,4*] (ORCID 0000-0002-1498-5707), Yinxin Dong[3,5,6] (ORCID 0000-0002-0187-4135), Frédéric Bouché[3,7] (ORCID 0000-0002-8017-0071), Ryland Bednarek[3,8], Mark Rowe[3], Thomas S. Ream[2,3,9], and Richard M. Amasino[1,2,3,*] (ORCID 0000-0003-3068-5402)

Affiliations:

[1] Laboratory of Genetics, University of Wisconsin, 425-G Henry Mall, Madison, WI 53706.

[2] United States Department of Energy Great Lakes Bioenergy Research Center, University of Wisconsin-Madison.

[3] Department of Biochemistry, University of Wisconsin, 433 Babcock Dr. Madison, WI 53706.

[4] Current Address: Plant Sciences Department, University of California-Davis, One Shields Ave., 104 Robbins Hall, Davis, CA 95616.

[5] College of Horticulture, Northwest A&F University, Yangling, Shaanxi 712100, China.

[6] Current Address: Key Laboratory for Plant Diversity and Biogeography of East Asia, Kunming Institute of Botany, Chinese Academy of Sciences, Kunming 650201, China.

[7] Current Address: Laboratory of Plant Physiology, University of Liege, Quartier Vallee 1 Sart Tilman Campus, Chemin de la Vallee n. 4, B-4000 Liege, Belgium.

[8] Current Address: Boyce Thompson Institute, Cornell University, 533 Tower Rd., Ithaca, NY 14853.

[9] Current Address: Monsanto Company, 700 Chesterfield Parkway West, Chesterfield, MO

[*]Correspondence to: danielwoods715@gmail.com and amasino@biochem.wisc.edu

Abstract: Perception of seasonal cues is critical for reproductive success in many plants. Exposure to winter cold is a cue that can confer competence to flower in the spring via a process known as vernalization. In certain grasses, exposure to short days is another winter cue that can lead to a vernalized state. In *Brachypodium distachyon*, we find that natural variation for the ability of short days to confer competence to flower is due to allelic variation of the florigen paralog *FT-like9* (*FTL9*). An active *FTL9* allele is required for the acquisition of floral

competence, demonstrating a novel role for a member of the florigen family of genes. Loss of the short-day vernalization response appears to have arisen once in *B. distachyon* and spread through diverse lineages indicating that this loss has adaptive value, perhaps by delaying spring flowering until the danger of cold damage to flowers has subsided.

Introduction

Many plants adapted to temperate climates have a biennial or winter-annual life history strategy. These plants become established in the fall, overwinter, and flower in the spring. Essential to this adaptive strategy is that flowering does not occur prior to winter and that the perception of winter leads to competence to flower in the spring (Woods et al., 2014). The winter cue perceived in many plants is exposure to a prolonged period of cold, and the process by which such exposure leads to competence to flower is known as vernalization (Chouard, 1960; Woods et al., 2014). In some plants, however, short days (SD) provide an alternative winter cue (Purvis and Gregory, 1937; Heide, 1994), and the process by which SD exposure leads to competence to flower has been referred to as SD vernalization (Purvis and Gregory, 1937). This phenomenon was called SD vernalization because a hallmark of cold-mediated vernalization is acquisition of *competence* to flower rather than flowering *per se*, and the SD-vernalization phenomenon is similar in that exposure to SD leads to competence, but plants must still be exposed to inductive LD to flower.

The physiology of SD vernalization has been studied extensively in rye, wheat, barley, and oat (Purvis and Gregory 1937; Dubcovsky et al.,2006; Sampson and Burrows 1972; Heide et al., 1994) although it exists in other families of plants as well (e.g., Chouard 1960). The study of SD vernalization in wheat and barley is complicated by the fact that there are genotypes of wheat

(e.g. Templar) and barley (e.g. Morex) in which flowering *per se* occurs in SD; i.e., certain wheat and barley genotypes are facultative LD plants in that they flower most rapidly in LD but also will flower in SD (Kikuchi et al., 2009; Caseo et al., 2011a; Evans et al., 1987). This SD flowering in wheat and barley is distinct from SD vernalization. *Brachypodium distachyon* (*B. distachyon*), however, is an obligate LD plant that only has a SD-vernalization pathway and not a SD-flowering pathway (Ream et al., 2014; Gordon et al., 2017; Woods et al., 2014); thus, the SD-vernalization pathway can be studied in *B. distachyon* without the complication of SD flowering.

Little is known at a molecular level about how the SD-vernalization pathway operates in any plant species, and thus we have explored the genetic basis of SD vernalization in *B. distachyon*. Our work reveals a novel role for a florigen family gene in the SD-vernalization pathway and provides a molecular explanation of the distinction between SD vernalization and SD flowering in the pooid grasses.

Results and Discussion

Natural Variation in the SD vernalization response in B. distachyon

The model pooid grass *B. distachyon* has a robust cold-mediated vernalization response (Ream et al., 2014; Gordon et al., 2017). To determine if any accessions also have a SD vernalization response, we grew 51 accessions in 8-hour SD followed by long days (LD; 16-h or 20-h) and, as controls, solely in LD or SD. Forty of the accessions exhibited a robust SD-vernalization response: these accessions flowered rapidly after the shift from SD to LD, but in LD alone flowering occurred only after quite long periods of growth, and the accessions never flowered in SD alone further confirming that *B. distachyon* is an obligate LD plant (Figure 1A

and B, Table S1 and S2, Figure 1-figure supplement 1; Materials and Methods contains the rationale for the controls). We refer to these 40 lines as SD-vernalization responsive and the 11 lines that did not have a SD vernalization response as SD-vernalization non-responsive.

Given that the longest days experienced in the native growth habitats of the *B. distachyon* accessions tested range between 15-16h (Figure 1-figure supplement 2), we evaluated whether the SD vernalization response was still effective when SD-grown accessions Koz3, TR12c and RON2 were shifted into a range of more native photoperiods (Figure 1D). Plants were grown in 8h SD for 9 weeks before shifting into 10, 12, 14, 15, or 16-h photoperiods (Figure 1D). All three SD-responsive accessions flowered more rapidly after exposure to SD when the length of day was 12-h or longer (Figure 1D). In *B. distachyon* 12-h is the minimal photoperiod that is still partially inductive for flowering (Ream et al., 2014; Woods et al., 2017). Thus, the flowering effect of SD vernalization is manifest at the same inductive photoperiods as cold-mediated vernalization.

To determine if SD vernalization, like cold-mediated vernalization, is a quantitative response, we conducted a SD-exposure time course. Four SD-responsive and 5 non-responsive accessions were grown for 2, 4, 6, 8, 10, or 12 weeks in 8-h SD before shifting into LD. Like cold-mediated vernalization, the SD response is quantitative—longer periods of SD exposure result in more rapid flowering in the SD-responsive accessions (Figure 1E; figure supplement 1). Furthermore, 8 weeks of SD exposure saturates the SD-vernalization response. Lastly, even 12 weeks of SD exposure did not enable flowering in any of the accessions we had characterized as SD non-responsive in the 8-week SD exposure evaluation noted above.

We also explored whether the SD vernalization response is possible at a range of developmental stages. In the experiments described above, the SD treatment started when

106 imbibed seeds were sown in soil and continued until plants were shifted into LD and, thus,
107 depending upon the length of time in SD, the SD treatment spanned a range of early
108 developmental stages. To determine if SD vernalization is effective at later developmental
109 stages, we grew SD-responsive accessions in LD for 2, 4, and 6 weeks and subsequently exposed
110 them to 8 weeks of SD. Plants were then returned to inductive LD to determine their SD
111 vernalization responsiveness. All of the SD vernalized plants flowered within 35 days after
112 shifting back into LD, forming 4 leaves on the parent culm in LD before flowering (Figure 1F;
113 Figure 1- figure supplement 1D, E), indicating the SD vernalization is equally effective at early
114 and later developmental stages.
115
116 *Genetic mapping of the SD vernalization response identifies an FT paralog*
117 To explore the genetic basis of natural variation in the SD-vernalization response, we
118 generated mapping populations from crosses between responsive and non-responsive accessions
119 (Koz3 X Bd1-1; 12c X Bd1-1; RON2 X Bd1-1; and Koz3 X 29-1; Figure 2-figure supplement
120 1). In all populations, SD responsiveness segregated as a single, dominant locus (Figure 2-figure
121 supplement 1A) that mapped as a large-effect QTL near the bottom of chromosome 2 (Figure 2-
122 figure supplement 1B). Fine mapping narrowed the interval to a region on chromosome 2
123 containing eight annotated genes (Figure 2-figure supplement 1C). None of these genes are
124 differentially expressed in the shoot apical meristem or leaf tissue of responsive versus non-
125 responsive lines grown in SD followed by LD, SD only, or LD only (data not shown), indicating
126 that the variant underlying this trait is not likely to be in a cis-regulatory region of a gene.
127 However, there is one nucleotide change in this interval present in all 11 SD non-responsive
128 accessions that is not found in any of the 40 SD-responsive accessions; this change results in a

129 threonine to lysine substitution at position 94 (T94K) in an *FT* paralog (Table S1-2; Figure 2-
130 figure supplement 2) referred to as *FT-like 9* (Bradi2g49795; *FTL9*) (Higgins et al., 2010; Figure
131 2-figure supplement 4). The founding member of this family is *FT* which encodes a small
132 protein, also known as 'florigen', that travels from leaves to the shoot apical meristem to induce
133 flowering (*e.g.*, (Corbesier et al., 2007; Tamaki et al.)).

134 Molecular analyses confirm that allelic variation at *FTL9* is responsible for natural
135 variation in the ability of SD exposure to confer competence to flower (Figure 2; Figure 2-figure
136 supplement 1). First, reducing *FTL9* expression in the SD-responsive accessions Koz3 and Bd21-
137 3 using artificial microRNAs (amiRNAs) eliminated the SD-vernalization response (Figure 2A
138 and Figure 2-figure supplement 1 D-I). However, the amiRNA lines remain fully responsive to
139 cold-mediated vernalization demonstrating that the role of *FTL9* is specific to the SD-
140 vernalization pathway (Figure 2B and Figure 2-figure supplement 1E-F). Second, constitutive
141 expression of an *FTL9* cDNA from the SD-responsive accessions Koz3 and Bd21 under the
142 control of the maize ubiquitin promoter in both SD-responsive (Bd21-3 and Koz3) and non-
143 responsive accessions (Bd29-1) caused transgenic plants to behave as if they were vernalized
144 without prior cold or SD treatment both in terms of accelerated flowering as well as expression
145 of *VERNALIZATION1* (*VRN1*) which is a marker of the vernalized state in grasses (Woods et al.,
146 2014) (Figure 2C and Figure 2-figure supplement 3). Furthermore, overexpression of *FTL9* does
147 not result in rapid flowering when plants are grown in SD whereas overexpression of *FT1* does
148 result in rapid flowering (Figure 2-figure supplement 3). The lack of rapid flowering in the *FTL9*
149 overexpression transgenics is consistent with the gene providing competence to flower rather
150 than flowering *per se*, whereas *FT1* expression directly induces flowering. In contrast,
151 constitutive expression of the *FTL9* cDNA from the SD-non-responsive accession Bd1-1 did not

affect the flowering behavior of transgenic lines (Figure 2C; Figure 2-figure supplement 3) indicating that the T94K change is likely to disrupt *FTL9* function consistent with the recessive nature of this allele (Figure 2-figure supplement 1A) and that the T94K change occurs in a highly conserved amino acid in this family of proteins in plants and animals (Figure 2-figure supplement 2B). In the experiments described above we evaluated transgenic expression of *FTL9* alleles from both Koz3 and Bd21-3 because *FTL9* alleles from SD-responsive accessions exhibit variation in the predicted C terminus of the FTL9 protein: the ancestral state of FTL9 is 178 amino acids, but in Koz3 there is a deletion of a single nucleotide (G) in amino acid 175 that alters the reading frame such that FTL9 is 184aa long. As noted above, both versions of *FTL9* confer competence to flower.

Characterization of FTL9 expression

Consistent with its role in SD vernalization, *FTL9* mRNA is barely detectable in LD, whereas its expression is 350-fold greater in SD (Figure 3A). When SD-grown plants are shifted to LD, *FTL9* mRNA expression declines to very low levels within a few days (Figure 3A). We tested whether the quantitative aspect of SD vernalization was correlated with changes in the expression of *FTL9*, but *FTL9* mRNA levels remained the same over 10 weeks of SD exposure (Figure 3-figure supplement 1D). Finally, *FTL9* exhibits a diurnal expression pattern in SD with mRNA levels increasing during the night to a peak at dawn and declining during the day to a minimum at dusk, *FTL9* expression remains low throughout a 20-h LD (Figure 3B and Figure 3-figure supplement 1A). However, when plants are shifted to free-run, constant-dark conditions, *FTL9* mRNA levels plummeted and did not oscillate, indicating that proper *FTL9* expression requires short day/long night cycles (Figure 3-figure supplement 1B).

176 *FTL9 is repressed in LD by VRN2*

177 Given the day-length dependence of *FTL9* expression, we analyzed its expression in a
178 *phyC-1* mutant background (Woods et al., 2014). In *phyC* the LD photoperiod flowering pathway
179 is abolished and mutant plants are extremely delayed in flowering and have the appearance of
180 SD-grown plants when grown under LD (Woods et al., 2014). Indeed, *FTL9* expression is
181 significantly elevated in *phyC* mutants grown in LD compared to wild type across all time points
182 tested (Figure 4E). Thus, certain PHYC-regulated genes may be negative upstream regulators of
183 *FTL9*. One candidate gene is *FT1*; in barley cultivars that can flower in SD, *HvFT1* has been
184 postulated to be a repressor of a closely related SD-expressed paralog of *FTL9* called *HvFT3*
185 (Figure 2-figure supplement 4) because relatively high *HvFT3* expression in SD precedes the
186 expression of *HvFT1* and, as *HvFT1* expression levels increase in SD, *HvFT3* expression
187 decreases (Kikuchi et al., 2009). The *FT1* expression pattern in wild-type and the *phyC* mutant is
188 consistent with a model in which FT1 represses *FTL9*: in the *phyC* mutant in LD, *FT1* is nearly
189 undetectable (Woods et al., 2014), and *FTL9*, as noted above, is highly expressed, whereas in
190 wild type *FT1* is expressed in LD and *FTL9* is not. To determine if *FT1* represses *FTL9* in *B*.
191 *distachyon*, we evaluated *FTL9* expression in *UBI:FT1* transgenic lines grown in SD, a condition
192 in which *BdFT1* is not expressed in wild-type plants. *FTL9* expression levels were similar
193 between *UBI:FT1* and wild-type (Figure 2-figure supplement 3H); thus, it is unlikely that *FT1*
194 acts as a LD repressor of *FTL9* in *B*. *distachyon*.

195 *VERNALIZATION2* (*VRN2*) is another candidate gene that might repress *FTL9* during LD
196 because *VRN2* expression is abolished in the *phyC* mutant (Woods et al., 2014) and the level of
197 *FTL9* expression is inversely correlated with the level of expression of *VRN2* (Figure 4A and
198 Figure 4-figure supplement 1A). *VRN2* is a flowering repressor, and its expression is a function

of day-length (Figure 4A and Figure 4-figure supplement 1A) (Dubcovsky et al., 2006; Woods et al., 2016). In LD, *VRN2* mRNA levels are elevated and *FTL9* mRNA is barely detectable, whereas in SD *VRN2* mRNA levels are low and *FTL9* is highly expressed (Figure 4-figure supplement 1A). When plants are shifted from SD to LD, *VRN2* levels rise to LD levels (Figure 4A), and *FTL9* expression subsides (Figure 3A). This expression pattern contrasts with that of *VRN2* in a SD-vernalization responsive variety of wheat in which *VRN2* levels remain at low SD levels after a shift to LD (Dubcovsky et al., 2006). In wheat, *VRN2* is down-regulated by both cold and short days suggesting that this gene might play a role in the integration of the SD vernalization and vernalization pathways (Dubcovsky et al., 2006). This is unlikely to be the case in *B. distachyon* as *VRN2* is up-regulated during the cold (Ream et al., 2014) and *VRN2* down-regulation in SD is not maintained during a SD-LD shift (Figure 4A).

That VRN2 controls *FTL9* expression in *B. distachyon* is supported by the upregulation of *FTL9* in LD when *VRN2* expression is suppressed by amiRNAs (Figure 4B and Figure 4-figure supplement 1B) and the lack of *FTL9* expression and lack of acquisition of competence to flower in SD when *VRN2* is constitutively expressed (Figure 4C-D and Figure 4-figure supplement 1C). Thus, *VRN2* is a repressor of flowering that creates a requirement for vernalization by suppressing flowering when the days are sufficiently long, and, when the day-length decreases below a threshold in winter, the lack of *VRN2* expression permits *FTL9* expression which leads to competence to flower. The regulation is one way: over- or under-expression of *FTL9* does not affect *VRN2* mRNA levels (Figure 2-figure supplement 3D).

The repression of *FT* family genes by LD-upregulated *VRN2* appears to be conserved in grasses. For example, in rice, in which SD are inductive for flowering, expression of the *VRN2* ortholog *GHd7* (Woods et al., 2016) is reduced in SD enabling expression of Hd3 which encodes

a florigen (Xue et al., 2008). Also, in wheat and barley, the florigen *FT3* is expressed in SD. This SD-specific expression of *FT3* results from the lower level of *VRN2* expression in SD (Kikuchi et al., 2009; Casao et al., 2011b).

Loss of the SD-vernalization response arose once in B. distachyon

Although all SD non-responsive accessions contain the T94K change at the *FTL9* locus, they do not cluster in a single group but rather are quite distantly related based on whole-genome analyses ((Gordon et al., 2017); Figure 2-figure supplement 5A) raising the possibility that the T94K allele arose independently more than once. However, a phylogenetic analysis focusing on the 65kb interval containing *FTL9* indicates that in all of the SD-non-responsive accessions the 65kb *FTL9* interval is highly conserved (Figure 2-figure supplement 5B) despite other regions of the genome being divergent. This suggests that the *FTL9* variant associated with loss of SD responsiveness arose only once and then spread by outcrossing to diverse accessions where it was maintained by positive selection. Although, *B. distachyon* is typically inbreeding, outcrossing occurs as well (Sancho et al., 2018).

The adaptive value of an active *FTL9* and a SD-vernalization response, which is the ancestral state, may be to ensure that vernalization occurs in mild climates in which SD may be a more reliable indicator of winter than cold. The adaptive value of loss of *FTL9* activity and the corresponding loss of the SD-vernalization response might be to enable *B. distachyon* to grow in regions with a more variable spring climate in which a robust SD-vernalization response might lead to flowering before the danger of a hard freeze, which would damage sensitive floral organs, had passed. Interestingly, the SD-non-responsive accessions also require a longer period of cold exposure than the SD-responsive accessions to become fully vernalized ((Gordon et al., 2017)

and Figure 1C; Table S3) which is consistent with the SD-non-responsive accessions having undergone adaptation for later spring flowering. Also, consistent with this hypothesis on the adaptive value of loss of *FTL9* activity, the non-responsive accessions tend to have been collected at higher latitudes than the responsive accessions (Figure 1-figure supplement 2); however, latitude is only one of many factors that may relate to the latest date of a damaging freeze.

Roles of SD expressed FT-like genes in grass flowering

FTL9 is part of a *FT*-like gene family that has expanded to 14 members in grasses ((Higgins et al., 2010) and Figure 2-figure supplement 4). The roles of the other *FT*-like genes in grasses have not been thoroughly explored. Studies in wheat and barley indicate that a candidate gene underlying a QTL that confers the ability of certain varieties to flower in SD (*Ppd-H2)* (Laurie et al., 1995) is likely a paralog of *FT* referred to as *FT3* (Faure et al., 2007; Kikuchi et al., 2009; Casao et al., 2011a). The dominant *FT3* allele, which enables SD flowering, is often found in spring barley cultivars grown in more southern latitudes, whereas the recessive allele is typically associated with winter cultivars grown in more northern latitudes (Casao et al., 2011a). *FT3* is implicated in actual flowering in SD in wheat and barley as opposed to the competence to flower in LD that is conferred by SD-specific expression of *FTL9* in *B. distachyon*. *FTL10* is the *B. distachyon* ortholog of wheat and barley *FT3* (Halliwell et al., 2016; Figure 2-figure supplement 4). *FTL10* and *FTL9* are closely related paralogs that resulted from a grass-specific duplication event, and thus *FTL10* and *FTL9* reside in sister clades (Figure 2-figure supplement 4). *FT3* is up-regulated in SD in barley and wheat, whereas *FTL10* expression in *B. distachyon* is not modulated by day-length and its expression level is quite low in all conditions tested (Figure

3D). However, constitutive expression of *FTL10* from the maize ubiquitin promoter results in flowering during transgenic line generation in tissue culture (Figure 3E) and rapid flowering in SD (Figure 2-figure supplement 3I, J) similar to the effects of expression of other *FT1* orthologs in *B. distachyon* (Figure 2-figure supplement 3I, J ; Ream et al., 2014) and wheat (Lv et al., 2014) indicating that *FTL10* has florigen activity. In contrast, as discussed above, constitutive expression of *FTL9* does not induce flowering in SD or in tissue culture which is consistent with its role in establishing competence to flower as opposed to the florigen-like role of *FTL10* in inducing flowering (Figure 2-figure supplement 3G, I, J).

Interestingly, like *FTL9* in *B. distachyon*, the *FTL9* ortholog in sorghum and maize called *CENTRORADIALIS 12* (*CN12*) (Figure 2-figure supplement 4, Figure 2-figure supplement 6; Murphy et al., 2011; Meng et al., 2011) is also expressed only in SD. However, in sorghum and maize, which are SD-flowering or day neutral plants, *CN12* along with *CN8* (the *FTL10*/*FT3* ortholog) are both florigenic (Meng et al., 2011; Lazakis et al., 2011). Thus, gene duplication of an ancestral SD-expressed *FT*-like gene at the base of the grass family appears to have resulted in the *FTL9*/*CN12* and *FTL10*/*FT3*/*CN8* clades (Figure 2-figure supplement 4). Grasses that are classified as SD plants like sorghum and photoperiodic maize (Murphy et al., 2011; Meng et al., 2011) are in fact SD plants because a florigenic member of one of the SD-expressed clades provides the primary florigen activity. Wheat and barley are LD plants because the strongest florigen activity is provided by LD-expressed *FT* family members in other clades such as *FT1*. However, many varieties of wheat and barley exhibit a facultative LD response—i.e., they also can flower in SD. The SD flowering of barley appears to result from expression of SD-induced clade members such as *FT3* (Kikuchi et al., 2009; Faure et al., 2007). All accessions of *B. distachyon* that we have analyzed are obligate LD plants because the florigenic member of the

clade, *FTL10*, is not expressed at sufficient levels to cause flowering in SD and the other member of the clade, *FTL9*, evolved the different function of providing competence to flower in pooid grasses rather than directly promoting flowering like it does in sorghum and maize.

SD-mediated vernalization was first described in rye in 1937 (Purvis and Gregory, 1937) and has been described in wheat and barley (Evans, 1987; Heide, 1994; Dubcovsky et al., 2006); however, sequence data available to date has not revealed a clear ortholog of *FTL9* in wheat or barley (Figure 2-figure supplement 4; Faure et al., 2007). It will be interesting to determine whether *FTL9* orthologs or other *FT* family members are involved in SD vernalization in cereals.

Gene duplication and divergence has enabled diverse roles for *FT* family members in flowering. The founding members of the *FT* family provide florigen activity (Corbesier et al., 2007; Tamaki et al.). In beet, an *FT* family member is an inhibitor of flowering that is key to establishing a requirement for vernalization. Our work in *B. distachyon* reveals a new role for an *FT* family member: the establishment of competence to flower without direct florigen activity.

Convergence between the SD vernalization and cold-mediated vernalization pathways

To explore the relationship between SD vernalization and the cold-mediated vernalization pathway, we evaluated the expression of the key flowering genes *VRN1* and *FT1* (known as *VRN3* in wheat, Yan et al., 2006) in SD, LD and during a SD-LD shift (Figure 5). *FT1* and *VRN1* are lowly expressed in SD only and LD only in Koz3 and Bd1-1 consistent with the delayed flowering phenotype of these accessions without prior SD or cold vernalization (Figure 5). However, prolonged exposure of Koz3 (SD vernalization responsive) to SD followed by a shift to LD (SD-LD) results in the up-regulation of both *FT1* and *VRN1*, whereas this treatment does not result in *FT1* and *VRN1* expression in the SD non-responsive accession Bd1-1 (Figure 5).

Thus, SD vernalization provides competence to flower by enabling the expression of *VRN1* and *FT1* once plants are in LD. As previously shown for cold-mediated vernalization (Woods et al., 2016), SD-mediated vernalization is attenuated in *amiVRN1* transgenic lines (Figure 5C, D), further corroborating that the cold- and SD-mediated vernalization pathways converge on enabling expression of genes like *VRN1* when plants are exposed to inductive LD. It is important to note that the loss of *FTL9* activity has no effect on cold-mediated vernalization (Figure 2) demonstrating that there are features that define the two pathways as separate. It will be interesting to determine mechanisms through which *FTL9* expression in SD enables an alternate path to cold-mediated vernalization to provide competence to flower. This competence is due, at least in part, by enabling *VRN1* expression to increase in LD. For example, *FTL9* may be involved in modifying *VRN1* chromatin during SD to allow its activation during LD. A similar model may apply to the cold-mediated vernalization pathway: for example, repression of *VRN1* before cold-mediated vernalization is associated with high levels of H3K27me3 at *VRN1* chromatin in both wheat and *B. distachyon* (Oliver et al., 2009; Woods et al., 2017).

SD-mediated vernalization in other groups of plants

Similar to cold-mediated vernalization, the SD-mediated vernalization response is found in an array of species spanning flowering plant diversification (Chouard, 1960; Heide et al., 1994). Advances in understanding the molecular underpinnings of cold-mediated vernalization in several different plant groups as well in paleobotany and earth climate history indicate that cold-mediated vernalization likely evolved independently multiple times as flowering plants were radiating some 140 million years ago (e.g., Bouche et al., 2017). The fact that *FTL9* appears to be grass-specific suggests that SD-mediated vernalization likely evolved independently several

337 times. It will be interesting to evaluate the molecular basis of SD-vernalization pathways in
338 different plant groups.
339
340 **Materials and Methods**
341 Growth Conditions and Plant Phenotyping
342 Seeds were imbibed overnight in distilled water at 5°C then grown in MetroMix 360 (Sungrow)
343 in 3-inch plastic pots under four 5000 K T5 fluorescent bulbs (300 mmol m^{-2} s^{-1} at plant level)
344 at 21-22°C during the light period and 18°C during the dark and fertilized weekly with Peters
345 Excel 15-5-15 Cal-Mag and Peters 10-30-20 Blossom Booster (RJ Peters). To minimize light
346 intensity differences, plant positions were rotated several times per week. Flowering time was
347 measured as the number of days from the emergence of the coleoptile to the day when
348 emergence of the spike was visible. The developmental stage of the plant was recorded as the
349 number of primary leaves derived from the parent culm at the time of heading. For all
350 experiments at least 6 plants were used to obtain the days to heading and leaf count averages.
351 Representative phenotyping results are presented, each of which were repeated in independent
352 experiments with similar results.
353
354 Marker Development
355 Development of indel markers (Table S4) was done using the sequenced genomes of Koz3, Bd1-
356 1, 12c, Bd29-1, and RON2 (Gordon et al., 2017). All markers are optimized to anneal at 51°C
357 and produce a product roughly 100bp in length. Markers were resolved using a 3% sodium
358 borate agarose gel.

Generation of *amiFTL9* and *UBIFTL9*, *UBIFTL10* Transgenic lines

amiRNAs specific for two distinct parts of the *FTL9* mRNA were designed using the amiRNA designer tool at wmd3.weigelworld.org based on MIR528 from rice in the pNW55 vector. Gateway-compatible *amiFTL9* PCR products were recombined into pDONR221 using Life Technologies BP Clonase II following the manufacturer's protocol. Clones were verified by sequencing. The pDONR221 vector containing the desired amiRNA in combination with another vector containing the maize ubiquitin promoter were both recombined into destination vector p24GWI (designed by Devin O'Connor at the Plant Gene Expression Center, Albany, CA) using Life Technologies LR clonase II plus following the manufacturer's protocol. Clones were verified by sequencing to ensure that the maize ubiquitin promoter was upstream from the amiRNA. The constructs were transformed into *A. tumefaciens* strain Agl-1. Plant callus transformation was as previously described (Vogel et al., 2008). Independent transgenic lines were genotyped for the transgene using an amiRNA forward primer specific for the targeted transcript and a reverse primer derived from the pNW55 backbone sequence (Table S5). Primers used to generate the amiRNAs are listed in Table S5.

FTL9 cDNAs were amplified from SD-grown Bd21, Koz3, and Bd1-1 plants. *FTL10* cDNAs were amplified from Bd21-3 grown in LD. cDNAs were gel extracted (Qiagen) and cloned using CloneJET PCR according to the manufacturer's protocol (Thermo Fischer Scientific). Clones were verified by sequencing. The cDNA was then subcloned using primers compatible with the Gateway BP clonase system according to the manufacturer's protocol (Thermo Fischer Scientific). The BP plasmid was verified by sequencing and then recombined into pANIC10A (Mann et al., 2012) using Life Technologies LR Clonase II following the manufacturer's protocol. Clones were verified by sequencing in pANIC10A and then transformed into

382 *Agrobacterium tumefaciens* strain Agl-1. Plant callus transformation was performed as described
383 (Vogel et al., 2008). Independent transgenic lines were genotyped for the transgene using a
384 cDNA-specific forward and pANIC vector AcV5 tag reverse primer (Table S5). Primer pairs
385 used to clone each cDNA are listed in Table S5.

386 RNA expression analysis and qPCR

387 RNA extraction and expression analysis were performed as described in (Ream et al., 2014).

388

389 QTL analysis

390 QTL analysis was performed as described in (Woods et al., 2017).

391

392 Phylogenetic and syntenic analyses

393 Phylogenetic analyses of *FT*-like genes were performed using both the full-length *FTL9* and *FT*
394 genes and the PEBP domains as seed sequences for BLAST searches using Phytozome and
395 NCBI as described in (Woods et al., 2011). Maximum-likelihood analyses were conducted using
396 SeaView 4.5.4 (Gouy et al., 2010). Phylogenetic analysis of the SD-vernalization interval across
397 51 *B. distachyon* accessions was done using variants called within a VCF file generated as in
398 (Gordon et al., 2017). Relationships among *B. distachyon* accessions based on the mapped
399 interval were determined using the TASSEL 5 software package (Bradbury et al., 2007). Synteny
400 in the chromosomal regions around *FTL9* of *Brachypodium distachyon*, *Oryza sativa*, *Seteria*
401 *italica*, *Sorghum bicolor*, *Panicum hallii*, and *Zea mays* was investigated using the GEvo
402 software package within CoGe (Lyons et al., 2008).

403 LD only and SD only controls for characterization of the SD-vernalization response.

To determine if prolonged growth in short days followed by a shift into long days (SD-LD) can promote flowering, we grew 43 delayed flowering accessions in 8-hour short days for 8 weeks before shifting into either 16 or 20-hour days (Table S1-2). The two controls for this experiment were accessions grown in SD and LD only. The SD only control demonstrates that growth in SD is indeed non-inductive for flowering because growth for 150 days does not permit flowering in any of the accessions tested (Table S1-2). Dissections on the parent culm revealed that the meristems were still vegetative after 150 days of growth in SD in all accessions tested, consistent with previous reports (Woods et al., 2014; Gordon et al., 2017). The LD only control was chosen to ensure that if robust flowering occurs following a shift from SD to LD, this was indeed due to the prior SD treatment and not simply due to the age of the plant when shifted into inductive LD. Thus, an accession is SD vernalization responsive if the SD-LD shifted plants flower much more rapidly than the LD only controls.

Control for day and night temperature during SD vernalization.

To ensure the acceleration of flowering by prolonged exposure to SD was indeed due to the shorter photoperiod and not due to extended periods of cooler dark temperatures of 18°C, we grew four accessions (KOZ3, 12c, RON2 and Bd18-1) in SD under constant day and night temperatures of 21°C. Accessions grown under constant 21°C day/night temperatures showed the same robust SD vernalization response as those grown under 21°C/18°C day/night temperatures (data not shown), indicating that the SD vernalization phenomenon is due strictly to the photoperiod and not a composite of photoperiod and temperature.

Acknowledgments: We thank John Vogel and Sean Gordon for leading the effort to sequence and analyze 51 *B. distachyon* genomes (Gordon et al., 2017) which provided data critical for this

work. We thank Jill Mahoy and Heidi Kaeppler for providing transgenic *B. distachyon* lines, and Scott Woody for many helpful suggestions on improving this manuscript. **Funding:** This work was funded in part by the National Science Foundation (IOS-1258126 to R.M.A.), the Great Lakes Bioenergy Research Center (Department of Energy Biological and Environmental Research Office of Science DE-FCO2-07ER64494), a National Institutes of Health-sponsored pre-doctoral training fellowship to the University of Wisconsin Genetics Training program to D.P.W., a Gordon and Betty Moore Foundation and the Life Sciences Research Foundation fellowship to support T.S.R., and a Wallonie-Bruxelles International fellowship to F.B.

Author Contributions: D.P.W., and R.M.A. conceived and designed research plans with assistance from T.S.R and F.B.; D.P.W. and Y.D. characterized the SD vernalization phenomenon across sequenced *B. distachyon* accessions; F.B. analyzed climate data; M.R. and D.P.W. developed markers and performed QTL analysis; R.B. and Y.D. cloned *FTL9* and phenotyped with D.P.W; D.P.W. prepared figures with input from F.B. and R.M.A.; D.P.W. and R.M.A. wrote the article with contributions and approval of all authors. **Competing Interests:** Authors declare no competing interests. **Data and materials availability:** All data us available in the main text or the supplementary materials.

Supplementary Materials:

Figures S1-S10

Tables S1-S5

References

449 **Bouché F, Woods DP, Amasino RM** (2017) Winter Memory throughout the Plant Kingdom:
450 Different Paths to Flowering. *Plant Physiology* **173**: 27–35

451 **Bradbury P, Zhang Z, Kroon DE, Casstevens TM, Ramdoss Y, Buckler ES** (2007)
452 *TASSEL*: Software for association mapping of complex traits in diverse samples.
453 *Bioinformatics* 23:2633-2635.

454 **Casao MC, Karsai I, Igartua E, Gracia MP, Veisz O, Casas AM** (2011a) Adaptation of
455 barley to mild winters: A role for *PPDH2*. *BMC Plant Biol* **11**: 164

456 **Casao MC, Igartua E, Karsai I, Lasa JM, Gracia MP, Casas AM** (2011b) Expression
457 analysis of vernalization and day-length response genes in barley (*Hordeum vulgare L.*)
458 indicates that *VRNH2* is a repressor of *PPDH2* (*HvFT3*) under long days. *Journal of*
459 *Experimental Botany* **62**: 1939–1949

460 **Chouard P** (1960) Vernalization and its relations to dormancy. *Annu Rev Plant Physiol* **11**: 191–
461 238

462 **Corbesier L, Vincent C, Jang S, Fornara F, Fan Q, Searle I, Giakountis A, Farrona S,**
463 **Gissot L, Turnbull C, et al** (2007) FT Protein Movement Contributes to Long-Distance
464 Signaling in Floral Induction of Arabidopsis. *Science* **316**: 1030–1033

465 **Dubcovsky J, Loukoianov A, Fu D, Valarik M, Sanchez A, Yan L** (2006) Effect of
466 Photoperiod on the Regulation of Wheat Vernalization Genes *VRN1* and *VRN2*. *Plant Mol*
467 *Biol* **60**: 469–480

468 **Evans LT** (1987) Short day induction of inflorescence initiation in some winter wheat varieties.
469 *Functional Plant Biol* **14**: 277–286

470 **Faure S, Higgins J, Turner A, Laurie DA** (2007) The *FLOWERING LOCUS T*-Like Gene
471 Family in Barley (*Hordeum vulgare*). *Genetics* **176**: 599–609

472 **Fjellheim S, Boden S, Trevaskis B** (2014) The role of seasonal flowering responses in
473 adaptation of grasses to temperate climes. *Front*. *Plant Sci*. **5**:431

474 **Gordon SP, Contreras-Moreira B, Woods DP, Marais Des DL, Burgess D, Shu S, Stritt C,**
475 **Roulin AC, Schackwitz W, Tyler L, et al** (2017) Extensive gene content variation in the
476 *Brachypodium distachyon* pan-genome correlates with population structure. *Nature*
477 *Communications* **8**: 2184

478 **Gouy M, Guindon S, Gascuel O** (2010) SeaView Version 4: A Multiplatform Graphical User
479 Interface for Sequence Alignment and Phylogenetic Tree Building. *Mol*. *Biol*. *Evol*. **27**, 221–
480 224

481 **Halliwell J, Borrill P, Gordon A, Kowalczyk R, Pagano ML, Saccomanno B, Bentley AR,**
482 **Uauy C, Cockram J** (2016) Systematic Investigation of *FLOWERING LOCUS T*-Like
483 Poaceae Gene Families Identifies the Short-Day Expressed Flowering Pathway Gene, *TaFT3*
484 in Wheat (*Triticum aestivum L.*). *Front Plant Sci* **7**: 1783–15

485 **Heide OM** (1994) Control of flowering and reproduction in temperate grasses. *New Phytol* **128**:
486 347–362

487 **Higgins JA, Bailey PC, Laurie DA** (2010) Comparative Genomics of Flowering Time
488 Pathways Using *Brachypodium distachyon* as a Model for the Temperate Grasses. PLoS
489 ONE **5**: e10065

490 **Kikuchi R, Kawahigashi H, Ando T, Tonooka T, Handa H** (2009) Molecular and Functional
491 Characterization of PEBP Genes in Barley Reveal the Diversification of Their Roles in
492 Flowering. *Plant Physiology* **149**: 1341–1353

493 **Lazakis CM, Coneva V, Colasanti J** (2011) ZCN8 encodes a potential orthologue of
494 Arabidopsis FT florigen that integrates both endogenous and photoperiod flowering signals
495 in maize. *Journal of Experimental Botany* **62**: 4833–4842

496 **Laurie DA, Pratchett N, Snape JW, Bezant JH** (1995) RFLP mapping of five major genes and
497 eight quantitative trait loci controlling flowering time in a winter x spring barley (*Hordeum*
498 *vulgare L.*) cross. Genome **38**: 575–585

499 **Lv B, Nitcher R, Han X, Wang S, Ni F, Li K, Pearce S, Wu J, Dubcovsky J, Fu D** (2014)
500 Characterization of *FLOWERING LOCUS T1* (*FT1*) Gene in Brachypodium and Wheat.
501 PLoS ONE **9**: e94171

502 **Lyons E, Freeling M,** (2008) How to usefully compare homologous plant genes and
503 chromosomes as DNA sequences. *Plant J*. **53,** 661–673

504 **Mann DGJ. *et al.*** (2012) Gateway-compatible vectors for high-throughput gene functional
505 analysis in switchgrass (*Panicum virgatum L.*) and other monocot species. *Plant Biotechnol*.
506 *J*. **10**, 226–236

507 **Meng X, Muszynski MG, Danilevskaya ON** (2011) The *FT*-like *ZCN8* gene functions as a
508 floral activator and is involved in photoperiod sensitivity in maize. *Plant Cell* **23**: 942–
509 960.

510 **Murphy RL, Klein RR, Morishige DT, Brady JA, Rooney WL, Miller FR, Dugas DV, Klein**
511 **PE, Mullet JE** (2011) Coincident light and clock regulation of *pseudoresponse regulator*
512 *protein 37* (*PRR37*) controls photoperiodic flowering in sorghum. *Proc Natl Acad Sci USA*
513 **108**: 16469–16474

514 **Oliver SN, FINNEGAN EJ, DENNIS ES, Peacock WJ, Trevaskis B** (2009) Vernalization-
515 induced flowering in cereals is associated with changes in histone methylation at the
516 *VERNALIZATION1* gene. *Proc Natl Acad Sci USA* **106**: 8386–8391

517 **Pin PA, Benlloch R, Bonnet D, Wremerth-Weich E, Kraft T, Gielen JJL, Nilsson O** (2010)
518 An Antagonistic Pair of *FT* Homologs Mediates the Control of Flowering Time in Sugar
519 Beet. *Science* **330**: 1397–1400

520 **Purvis ON, Gregory FG** (1937) Studies in Vernalisation of Cereals. Annals of Botany **1**: 1–26

Ream TS, Woods DP, Amasino RM (2012) The molecular basis of vernalization in different plant groups. *Cold Spring Harb Symp Quant Biol* **77**: 105–115

Ream TS, Woods DP, Schwartz CJ, Sanabria CP, Mahoy JA, Walters EM, Kaeppler HF, Amasino RM (2014) Interaction of Photoperiod and Vernalization Determines Flowering Time of *Brachypodium distachyon*. *Plant Physiology* **164**: 694–709

Sampson, D. R., and Burrows, V. D. (1972). Influence of photoperiod, short-day vernalization, and cold vernalization on days to heading in *Avena* species and cultivars. *Can. J. Plant Sci*. 52, 471–482.

Sancho R, Cantalapiedra C, Lopez-Alvarez D, Gordon S, Vogel J, Catalan P, Contreras-Moreira B (2018) Comparative plastome genomics and phylogenomics of *Brachypodium*: flowering time signatures, introgression and recombination in recently diverged ecotypes. *New Phytologist*. **218,** 1631-1644

Sasani S, Hemming MN, Oliver SN, Greenup A, Tavakkol-Afshari R, Mahfoozi S, Poustini K, Sharifi HR, Dennis ES, Peacock WJ, et al (2009) The influence of vernalization and daylength on expression of flowering-time genes in the shoot apex and leaves of barley (Hordeum vulgare). Journal of Experimental Botany **60**: 2169–2178

Tamaki S, Matsuo S, Wong HL (2007) Hd3a protein is a mobile flowering signal in rice. *Science*. ***316,*** 1033-1036

Trevaskis B, Hemming MN, Dennis ES, Peacock WJ (2007) The molecular basis of vernalization-induced flowering in cereals. *Trends in Plant Science* **12**: 352–357

Vogel J, Hill T (2008) High-efficiency Agrobacterium-mediated transformation of *Brachypodium distachyon* inbred line Bd21-3. *Plant Cell Reports*. **27**, 471–478

Whittaker C, Dean C (2017) The *FLC* Locus: A Platform for Discoveries in Epigenetics and Adaptation. Annu Rev Cell Dev Biol **33**: 555–575

Woods DP, Hope, CL, Malcomber, ST (2011) Phylogenomic analyses of the *BARREN STALK1/LAX PANICLE1* (*BA1/LAX1*) genes and evidence for their roles during axillary meristem development. *Mol. Biol. Evol*. **28**, 2147–2159

Woods DP, Ream TS, Amasino RM (2014) Memory of the vernalized state in plants including the model grass *Brachypodium distachyon*. *Front Plant Sci* **5**: 99

Woods DP, Ream TS, Minevich G, Hobert O, Amasino RM (2014) PHYTOCHROME C is an essential light receptor for photoperiodic flowering in the temperate grass, *Brachypodium distachyon*. Genetics **198**: 397–408

Woods DP, Bednarek R, Bouché F, Gordon S, Vogel J, Garvin D, Amasino RM (2017) Genetic Architecture of Flowering-Time Variation in *Brachypodium distachyon*. *Plant Physiology*. **173**, 269–279

Woods DP, Ream TS, Bouché F, Lee J, Thrower N, Wilkerson C, Amasino RM (2017) Establishment of a vernalization requirement in *Brachypodium distachyon* requires *REPRESSOR OF VERNALIZATION1*. *Proc Natl Acad Sci USA*. **25**, 6623-6628

Xue W, Xing Y, Weng X, Zhao Y, Tang W, Wang L, Zhou H, Yu S, Xu C, Li X, et al (2008) Natural variation in *Ghd7* is an important regulator of heading date and yield potential in rice. *Nat Genet* **40**: 761–767

Yan L, Loukoianov A, Tranquilli G, Helguera M, Fahima T, Dubcovsky J (2003) Positional cloning of the wheat vernalization gene VRN1. Proc Natl Acad Sci USA **100**: 6263–6268

Yan L, Fu D, Li C, Blechl A, Tranquilli G, Bonafede M, Sanchez A, Valarik M, Yasuda S, Dubcovsky J (2006) The wheat and barley vernalization gene *VRN3* is an orthologue of *FT*. Proc Natl Acad Sci USA **103**: 19581–19586

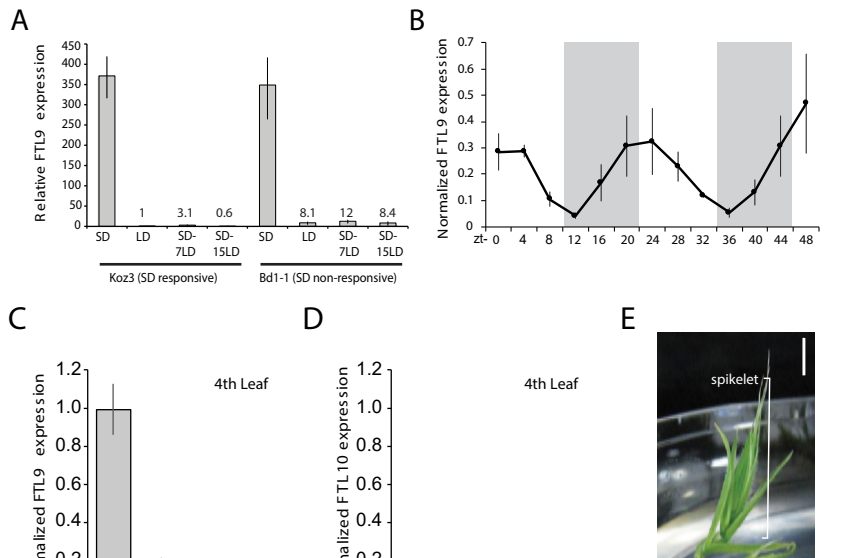

Fig. 3. *FTL9* expression is SD specific and diurnally fluctuating whereas *FTL10* expression is not influenced by day-length and encodes a florigenic protein.
(A) *FTL9* mRNA levels in Koz3 and Bd1-1 grown solely in 8h SD, solely in 20h LD, or 7 or 15 days after a shift from 8 weeks in SD to LD. RNA was prepared from newly expanded leaves on the parent culm. (B) Diurnal *FTL9* mRNA fluctuations in 8-h SD. Plants were grown in SD until the fourth-leaf stage was reached at which point newly expanded leaves were harvested every 4 hours throughout a 48-h diurnal cycle. Shaded boxes represent dark periods. (C) *FTL9* and (D) *FTL10* mRNA levels in 8, 12, 16, and 20-h photoperiods. Koz3 was grown to the four-leaf stage and newly expanded leaves were harvested in the middle of the photoperiod. (E) Representative image of T0 generation *UBI:FTL10* plants showing rapid spikelet formation (bracket) on callus regeneration media. All 15 independent *UBI:FTL10* calli flowered rapidly in regeneration media. Those plants without the transgene did not flower rapidly. *UBI:FTL10* T1 generation days to heading and leaf count data see Fig. S4I-J. Bar=.5cm. (A-D) Values represent the average of three biological replicates +/- standard deviation (4 leaves per replicate). Similar results were obtained in independent experiments. Gene expression was normalized to *UBC18* as described in (Ream et al., 2014).

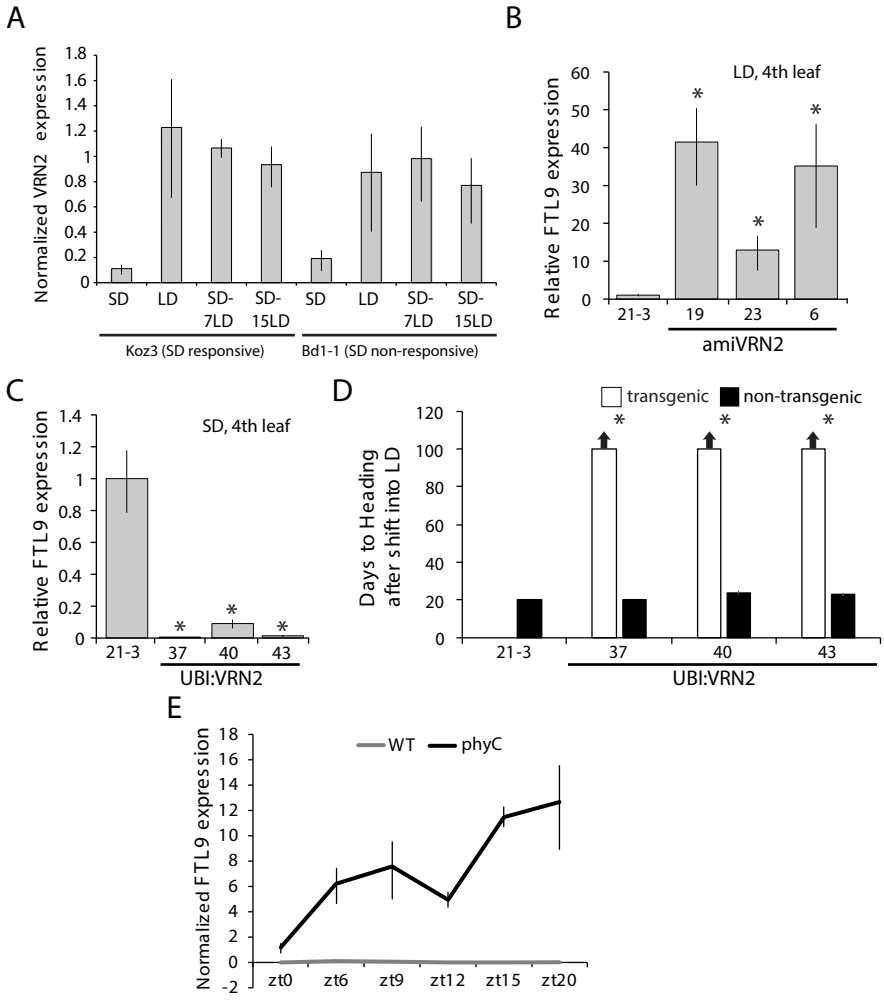

Fig. 4. *VRN2* represses *FTL9* in LD.
(A) *VRN2* is most highly expressed in LD. *VRN2* mRNA levels in Koz3 and Bd1-1 grown solely in 8h SD, solely in 20h LD only, or 7 and 15 days after a shift from SD to LD. Samples as described in Fig. 3A. (B) *FTL9* is expressed in LD when *VRN2* expression is reduced. *FTL9* mRNA levels were assessed by qRT-PCR in samples from a newly expanded leaf of Bd21-3 and *amiVRN2* plants at the fourth-leaf stage grown in 16-h LD. (C) *FTL9* expression is reduced in SD if *VRN2* is constitutively expressed. *FTL9* mRNA levels were determined as in B. (B,C) Average relative *FTL9* expression is shown for four biological replicates +/- standard deviation (4 leaves per replicate). Asterisk indicates a P-value <.05. See Figure 4-figure supplement 1 for *VRN2* expression. (D) Constitutive *VRN2* expression blocks the SD vernalization response. Days to heading for 3 independent *amiVRN2* transgenic lines (white bars) grown in SD for 10 weeks before shifting to 14h LD; wt Bd21-3 and segregating non-transgenic plants (black bars) show a normal SD vernalization response. Bars represent the average of 12 plants +/- standard deviation. (E) Gene expression of *FTL9* in Bd21-3 (grey line) and *phyC* (black line; *phyC-1* allele was used). Plants were grown in LD (20-hr days) until the fourth leaf stage was reached at which point the newly expanded fourth leaf was harvested at zt0, zt6, zt9, zt12, zt15 and zt20. The average of three biological replicates are shown +/- standard deviation (three leaves per replicate).

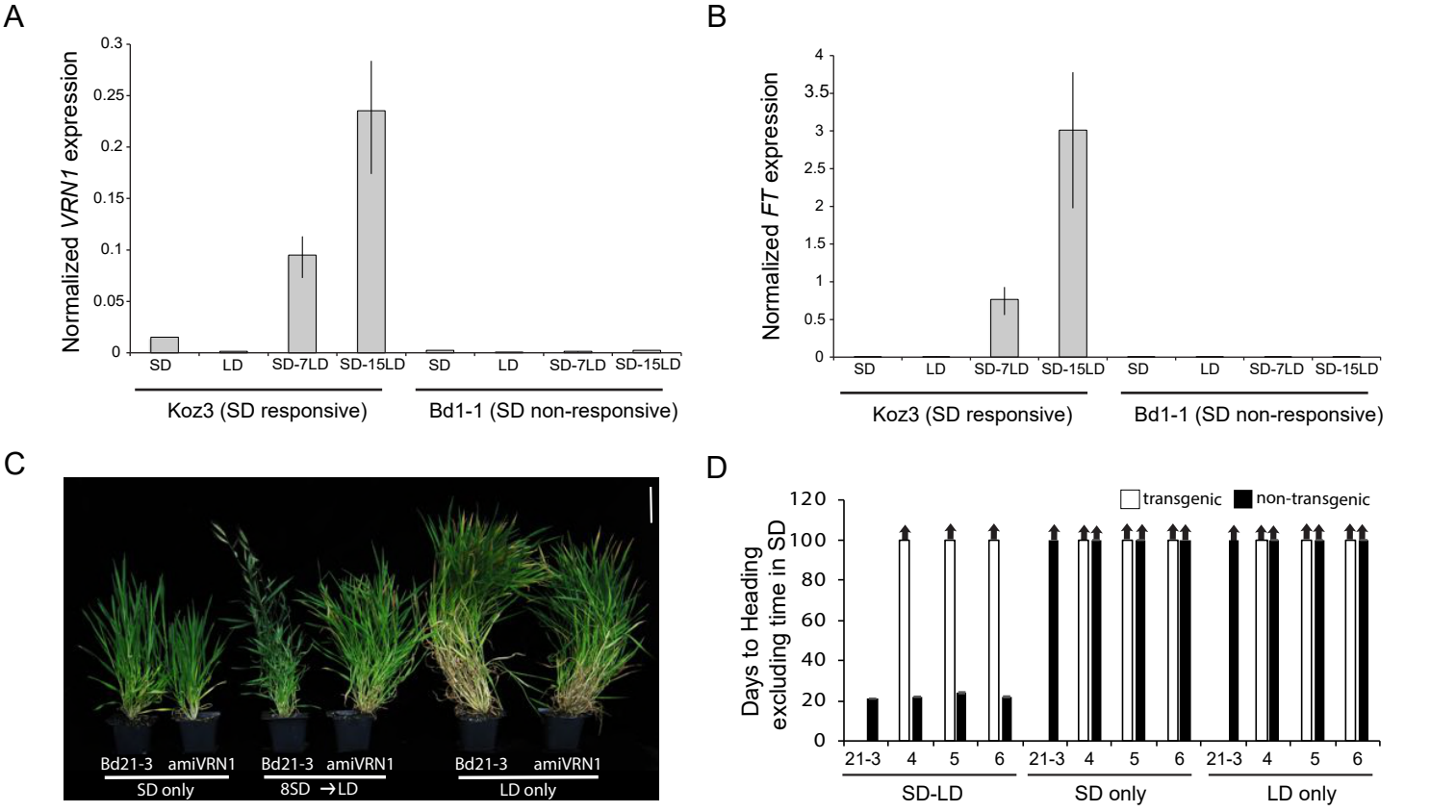

Fig. 5. SD vernalization induces the floral promoting genes *FT1* and *VRN1* in LD and the SD vernalization response depends on *VRN1* expression.
(A) *FT* and (B) *VRN1* mRNA levels in Koz3 and Bd1-1 grown solely in 8h SD, solely in 20h LD, or 7 or 15 days after a shift from 8 weeks in SD to LD. RNA was prepared from newly expanded leaves on the parent culm. Values represent the average of three biological replicates +/- standard deviation (4 leaves per replicate). The experiment was repeated with similar results. Expression normalized to *UBC18* as in Ream et al., 2014. (C) Knockdown of *VRN1* expression blocks the SD vernalization response. Representative photo of Bd21-3 wild-type, and *amiVRN1* grown in 8-h photoperiod (SD) only, 14-h photoperiod (LD) only and after a shift from 8 weeks in SD to LD. Bar=5cm. (D) Days to heading for 3 independent *amiVRN1* transgenic lines (4,5,6; white bars) grown in SD for 10 weeks before shifting to 14h LD; wt Bd21-3 and segregating non-transgenic plants (black bars) show a normal SD vernalization response. Bars represent the average of 12 plants +/- standard deviation.

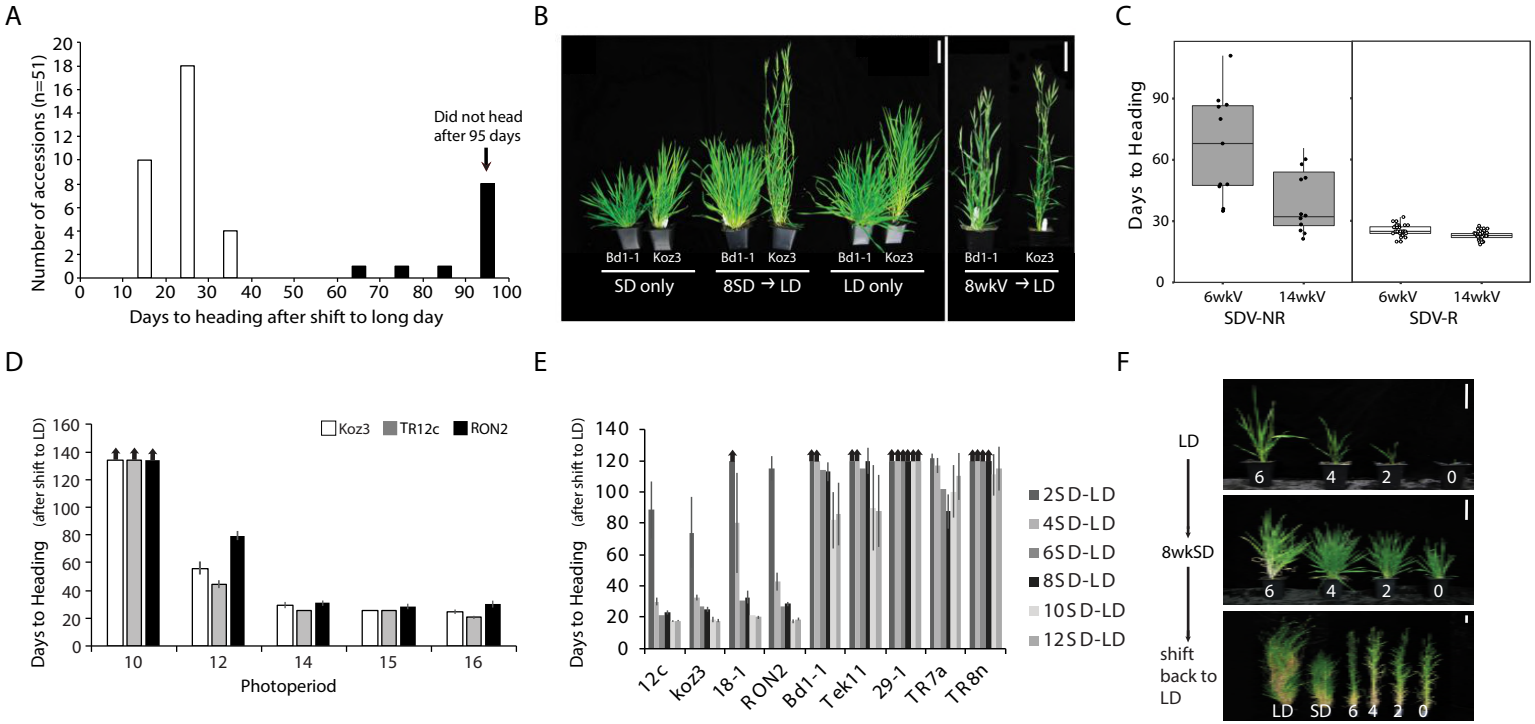

Figure 1. Natural variation in the short-day (SD) vernalization response in B. distachyon .
(A) SD vernalization response in 51 accessions that require cold mediated vernalization. Plants were grown for 56 days in 8h SD before the shift into long days (LD) of 14h or 16h. Day temperature of 21°C and night temperature of 18°C. SD vernalization is equally effective when day and night temperatures are constant (see materials and methods for details). White bars indicate accessions that are SD vernalization responsive and black bars accessions that are SD vernalization non-responsive. (B) Image of a representative SD vernalization responsive accession Koz3 and a SD vernalization non-responsive accession Bd1-1 taken after 100 days of growth. Only Koz3 flowers after the SD to LD shift whereas both accessions flower rapidly if exposed to 8 weeks of cold (8wkV) prior to growth in 16h LD. (C) Box plot illustrating that SD vernalization non-responsive accessions (SDV-NR, black dots) require longer periods of cold exposure to flower rapidly in 16h LD relative to SD vernalization responsive (SDV-R, white dots) accessions. The difference between SDV-NR and SDV-R flowering after vernalization is statistically significant. See supplemental Table S1-2 for days to heading, leaf count and standard deviation data for SD vernalization and Table S3 for days to heading data for 6 and 14 weeks of vernalization (6wkV and 14wkV). Bar=5cm (D) Short day vernalization response in three delayed-flowering accessions Koz3, TR12c and RON2 when shifted into 10, 12, 14, 15, and 16-h days. In this experiment, LD only and SD only control plants flowered similar to those in Table S1-2 (data not shown). Arrows indicate treatments in which plants did not flower within the experiment. Bars represent the average days to heading of 12 plants for each treatment. (E) SD vernalization time course. See Figure 1-figure supplement1B for SD and LD only controls and Figure 1-figure supplement1C for representative photo of plants at the end of the experiment. (F) The SD vernalization response is effective at multiple developmental stages. Koz3 and Tr12c were grown for 6, 4, 2, 0 weeks under 16-h LD before shifting into 8 weeks of 8-h SD (8wkSD). After the SD treatment plants were shifted back into LD. Representative photo of Koz3 taken after 40 days. See Figure 1-figure supplement1D, E for days to heading and leaf count data.

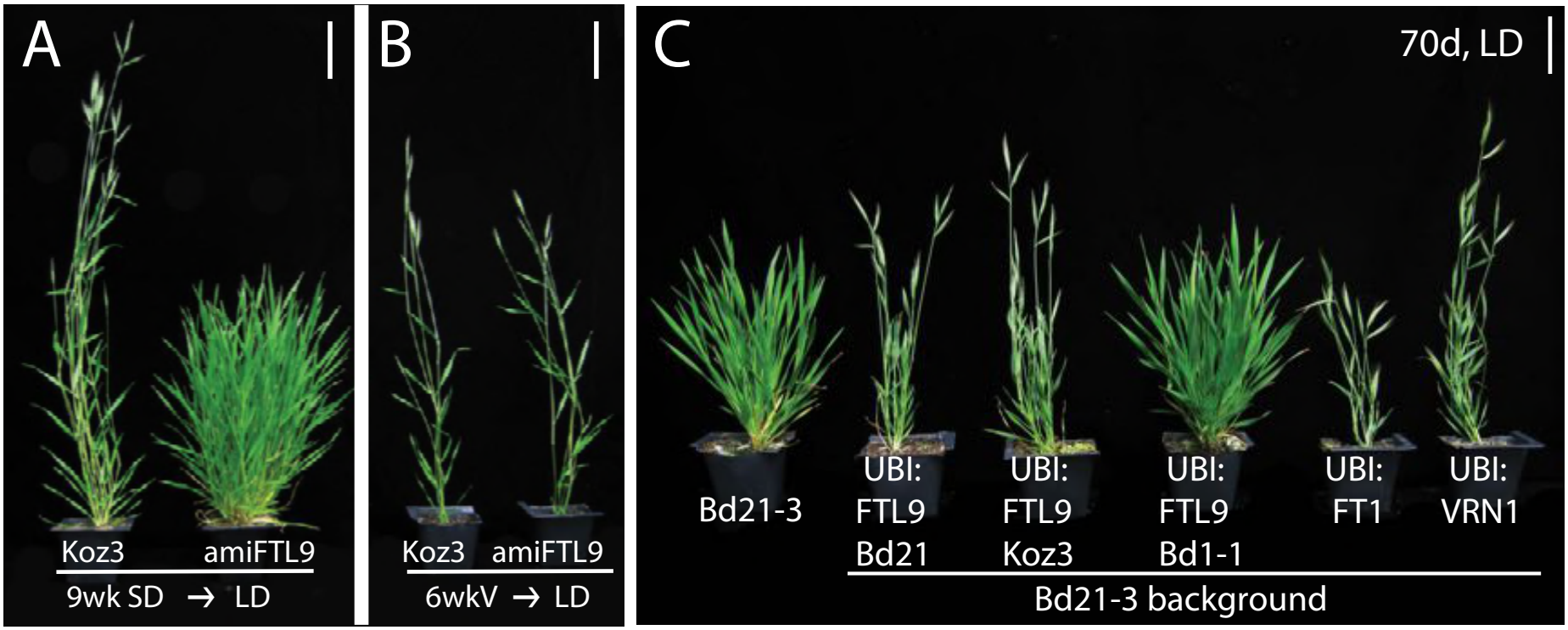

Figure 2. FTL9 is necessary for the SD vernalization response and sufficient to confer competence to flower.

(A) amiFTL9 knockdown prevents SD vernalization. Koz3 wild-type and amiFTL9 knockdown plants grown in 8h SD for 9 weeks (9wk SD) before shifting into 20h LD. Bar= 5cm. (B) amiFTL9 knockdown has no effect on cold-mediated vernalization. Plants were vernalized as imbibed seed at 5°C for 6 weeks (6wkV) before outgrowth in 20h LD. Bar= 5cm. See Figure 2-figure supplement 1 for amiFTL9 details. All experiments were repeated with similar results. (C) Constitutive expression of dominant FTL9 alleles permits flowering in LD. Representative photo of Bd21-3 wild-type, UBI:FTL9 Bd21 (FTL9 from Bd21), UBI:FTL9 Koz3 (FTL9 from Koz3), UBI:FTL9 Bd1-1 (FTL9 from Bd1-1), UBI:FT1 , and UBI:VRN1 grown in a 16-h photoperiod (LD) without cold or short day vernalization. All over expression lines are in the Bd21-3 background. Bar=5cm. See Figure 2-figure supplement 3 for UBI:FTL9 details including days to heading, leaf count data as well as mRNA expression analyses.

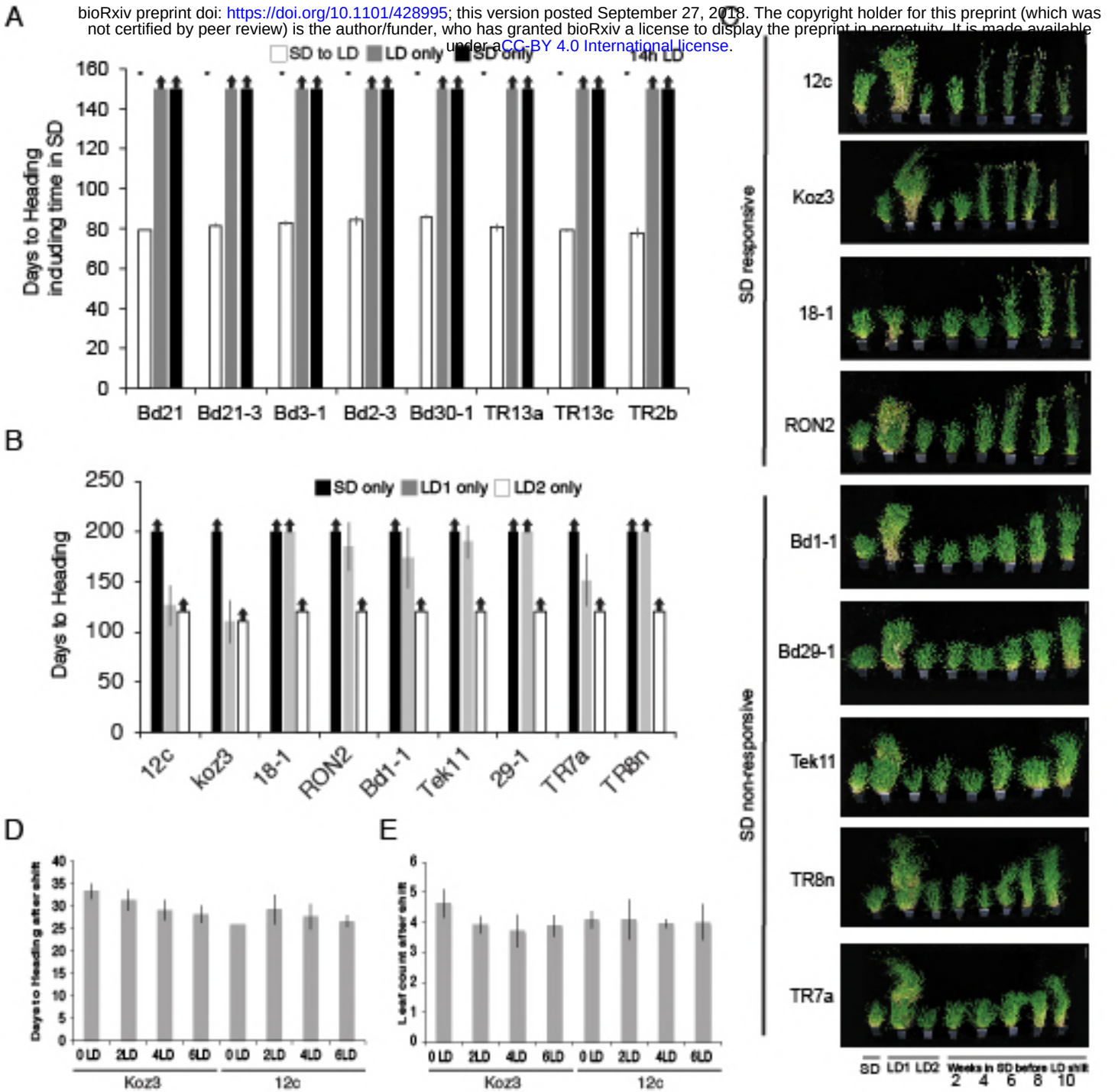

Figure 1-figure supplement 1. Natural variation in the short day vernalization response
(**A**) Short day vernalization response in eight accessions which flower rapidly in 20h or 16h daylengths, but which require vernalization when grown in a 14h daylength. White bars represent plants grown in 8h short days for 8 weeks before shifting into 14h long days (14h LD). Grey bars represent control plants grown solely in 14h LD (LD only) for the duration of the 150-day experiment and black bars represent control plants grown solely in 8h short days (SD only) for the duration of the experiment. Asterisks indicate statistically significant differences between SD to LD and LD only control plants ($p<0.05$). Arrows indicate treatments in which plants did not flower within the 150-d experiment. Bars represent the average days to heading of 12 plants for each treatment. (**B**) Days to heading of SD and LD only controls for the multiple developmental stages experiment. LD1, 20-h days for the full duration of the experiment. LD2, 20-h days but planted once all SD treated plants were shifted into LD. (**C**) Representative photographs of plants at the end of SD exposure time course experiment. LD1, 20-h days only for the full duration of the experiment. LD2, 20-h days but planted once all SD treated plants were shifted into LD. Bar=12cm. (**D**) Days to heading after shift into LD (**E**) Number of leaves formed on the parent culm after plants shifted into LD and flowered.

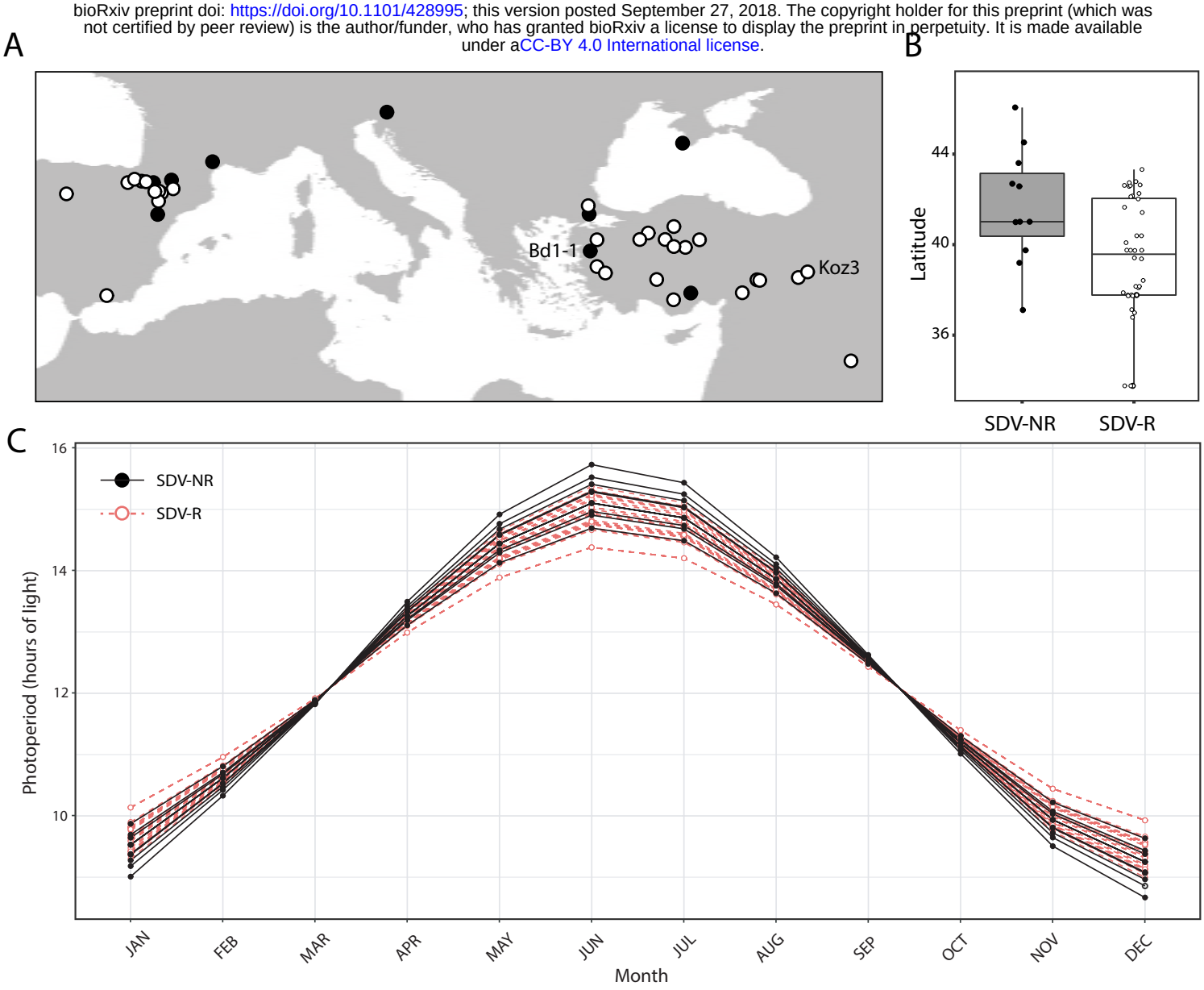

Figure 1-supplement figure 2. Geographical distribution of *B. distachyon* accessions used in this study. (**A**) Black dots represent SD vernalization-non-responsive accessions and white dots represent SD vernalization-responsive accessions. (**B**) Box plot indicating latitudinal distribution of SD vernalization non-responsive (SDV-NR; gray bar) and SD vernalization responsive (SDV-R; white bar) accessions. The difference is significant ($P<0.05$). (**C**) Photoperiod throughout a year for each accession used in this study in their native habitat.

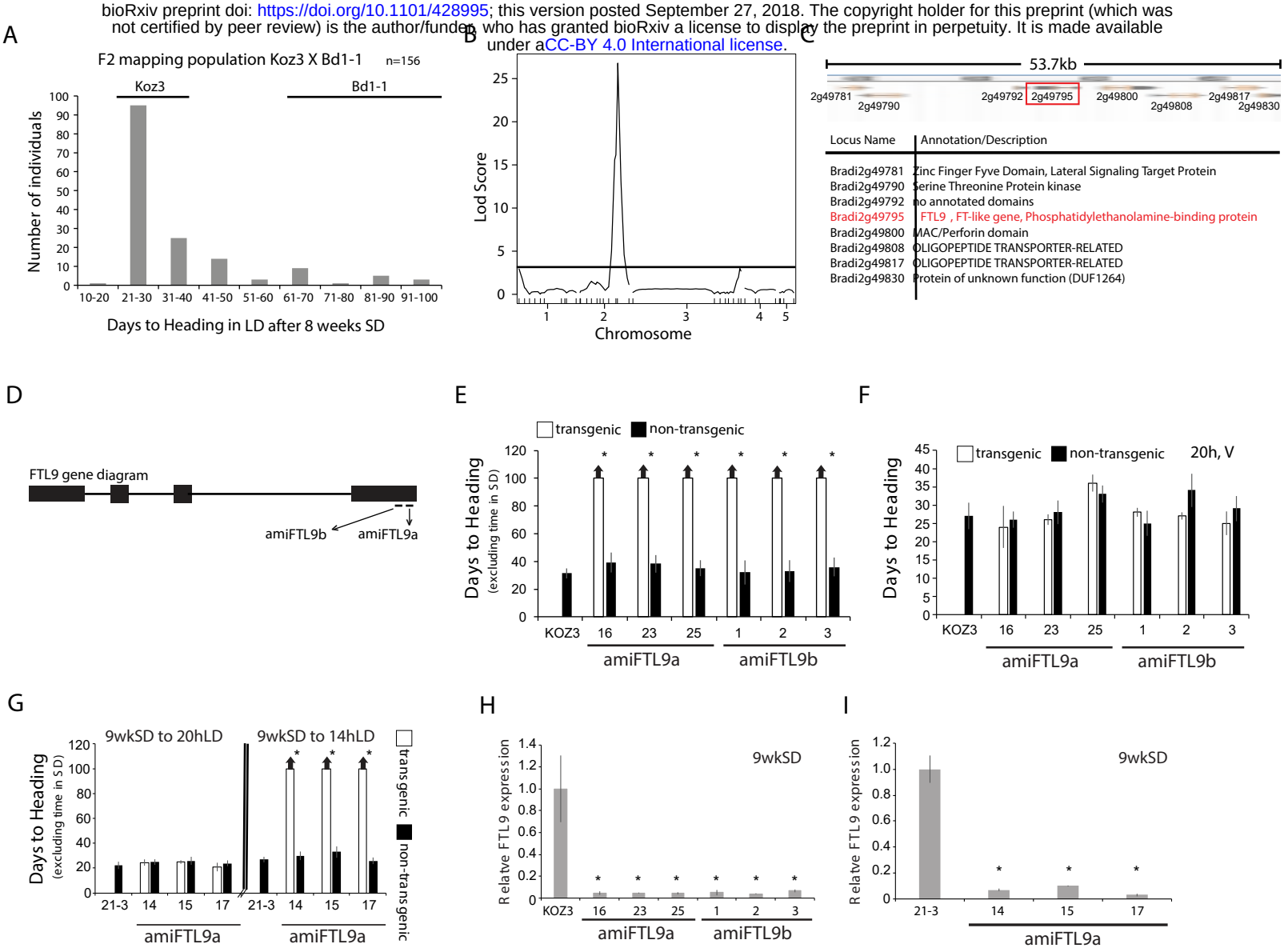

Figure 2- figure supplement 1. Identification of the *FT*-like paralog *FTL9* as essential for SD vernalization.
(A) Koz3 X Bd1-1 F2 mapping population. The F2 population was grown in 8h SD for 8 weeks before shifting into 20h LD. Days to heading does not include the time the population was in SD. Koz3 and Bd1-1 controls (grown in LD only) flowered as indicated above bars. (B) To identify regions of the *B. distachyon* genome contributing to the flowering variation in the F2 mapping population from (A), we performed a QTL analysis. Phenotypic data was correlated to genotypic data using 38 indel markers (see Table S4 for primer information and Data S1 for the phenotypic and genotypic data sets). A single, large-effect peak was detected at the bottom of chromosome 2. (C) Diagram of the 53.7kb interval containing the QTL using version 3.1 of the *B. distachyon* genome indicating 8 annotated genes within the interval. (D) Gene structure of *FTL9* showing the location of two amiRNA (*amiFTL9a* and *amiFTL9b*) targets in the 3' region of the gene. We targeted two different areas within the *FTL9* gene to control for off-target microRNA effects. (E) Days to heading of Koz3, three independent T1 *amiFTL9* transgenics (black bars), and non-transgenic sibling plants (white bars) grown in 20h days after exposure to 9 weeks of 8h SD. (**F**) Days to heading of Koz3, *amiFTL9* transgenics, and the non-transgenic sibling plants vernalized as imbibed seed for 4 weeks at 5C before outgrowth in 20h. (G) Days to heading of Bd21-3, three independent T1 *amiFTL9* transgenics (black bars), and non-transgenic sibling plants (white bars) grown in 20h and 14h. Bd21-3 does not have a vernalization requirement when grown under 20h light but does under 14h. For E,F, and G arrows above bars indicate that none of the plants flowered at the end of the experiment. (H-I) qRT-PCR of *FTL9* expression in *amiFTL9* confirming the knock down of *FTL9* expression in 8h SD. The newly formed ninth leaves on the parent culm were harvested either when the plants were at the ninth leaf stage or after 9 weeks of growth in 8h SD (9wkSD). Note the expression of the closely related paralog of *FTL9*, *FTL10* was not affected by the amiRNA nor was *VRN2* expression (data not shown). Asterisks above bars indicate statistically significant differences between *amiFTL9* transgenic and either wildtype or non-transgenic sibling plants (* P<0.05).

A

Gene ID	Koz3 /SD vern. responsive (CDS variants)	Bd1-1/SD vern. non-responsive (CDS variants)
Bradi2g49781	2 non-syn; (29/40 1st variant, 31/40 2nd variant)	0 variants
Bradi2g49790	0 variants	0 variants
Bradi2g49792	0 variants	0 variants
Bradi2g49795	1 frameshift (29/40 have frameshift)	2 non-syn; (2/11 1st variant, 11/11 2nd variant)
Bradi2g49800	1 non-syn (29/40 have non-syn)	0 variants
Bradi2g49808	1 non-syn, (31/40 have non-syn)	0 variants
Bradi2g49817	0 variants	0 variants
Bradi2g49830	1 non-syn (27/40 have non-syn)	0 variants

B

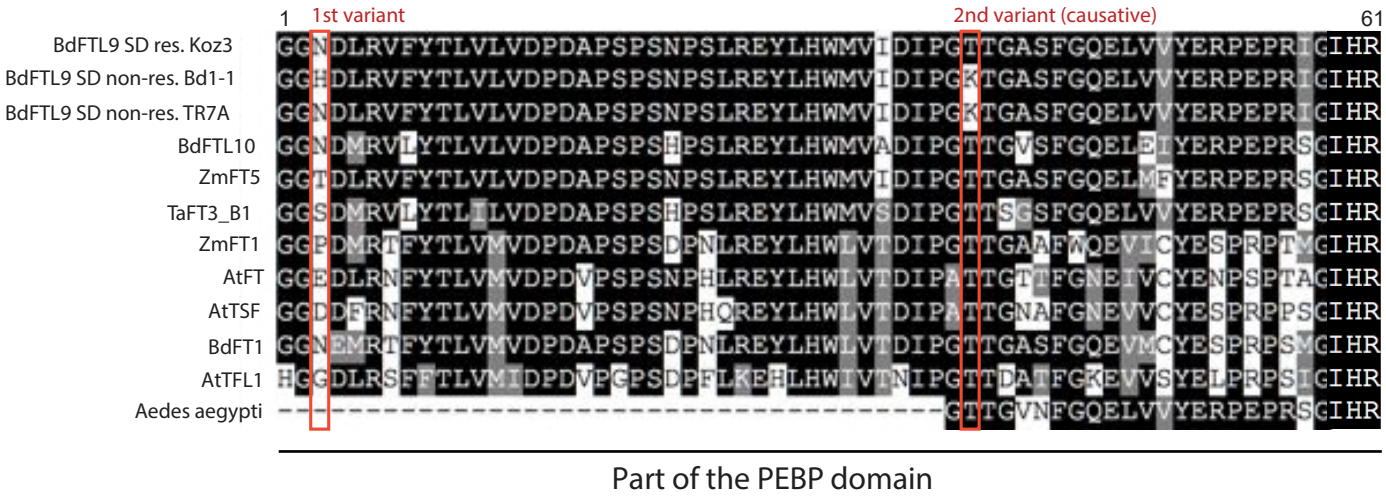

Figure 2-figure supplement 2. Coding variant summary within the SD vernalization mapped interval between SD vernalization responsive and non-responsive accessions

(A) List of non-synonomous variants (non-syn) or frameshifts that occur in the coding (CDS) region of all annotated genes within the 53.7kb mapped interval between Koz3 and Bd1-1 and the remaining 49 *B. distachyon* accessions that have been sequenced (Gordon et al., 2017). In parentheses is the prevalence of that variant across the 40 SD responsive accessions or the 11 SD non-responsive accessions. For a complete list of all variants (intronic, UTR, and intergenic) in the genes within the mapped interval see Data S2. The putative causative variant is in red. Variants within the full genomic sequence of *FTL9* were confirmed in all 51 sequenced accessions by Sanger sequencing. (**B**) Alignment of part of the phosphatidylethanolamine-binding domain in *FT*-like genes including the ligand-binding motif. The red boxes denote the two non-synonomous variants present in Bd1-1 not found in SD vernalization responsive accessions such as Koz3. The N to H change (1st variant) is not found across all SD non-responsive accessions and the amino acids at that position are highly variable across *FT*-like genes. In contrast, the T to K change (2nd variant, causative) in Bd1-1 is present in all SD non-responsive accessions and is in an amino acid that is highly conserved in other PEBP containing genes spanning plants and animals (*Aedes aeygypti*, a mosquito species, shown as an animal example). Bd= *Brachypodium distachyon*, Zm= *Zea mays*, Ta= *Triticum aestivum*, At= *Arabidopsis thaliana*.

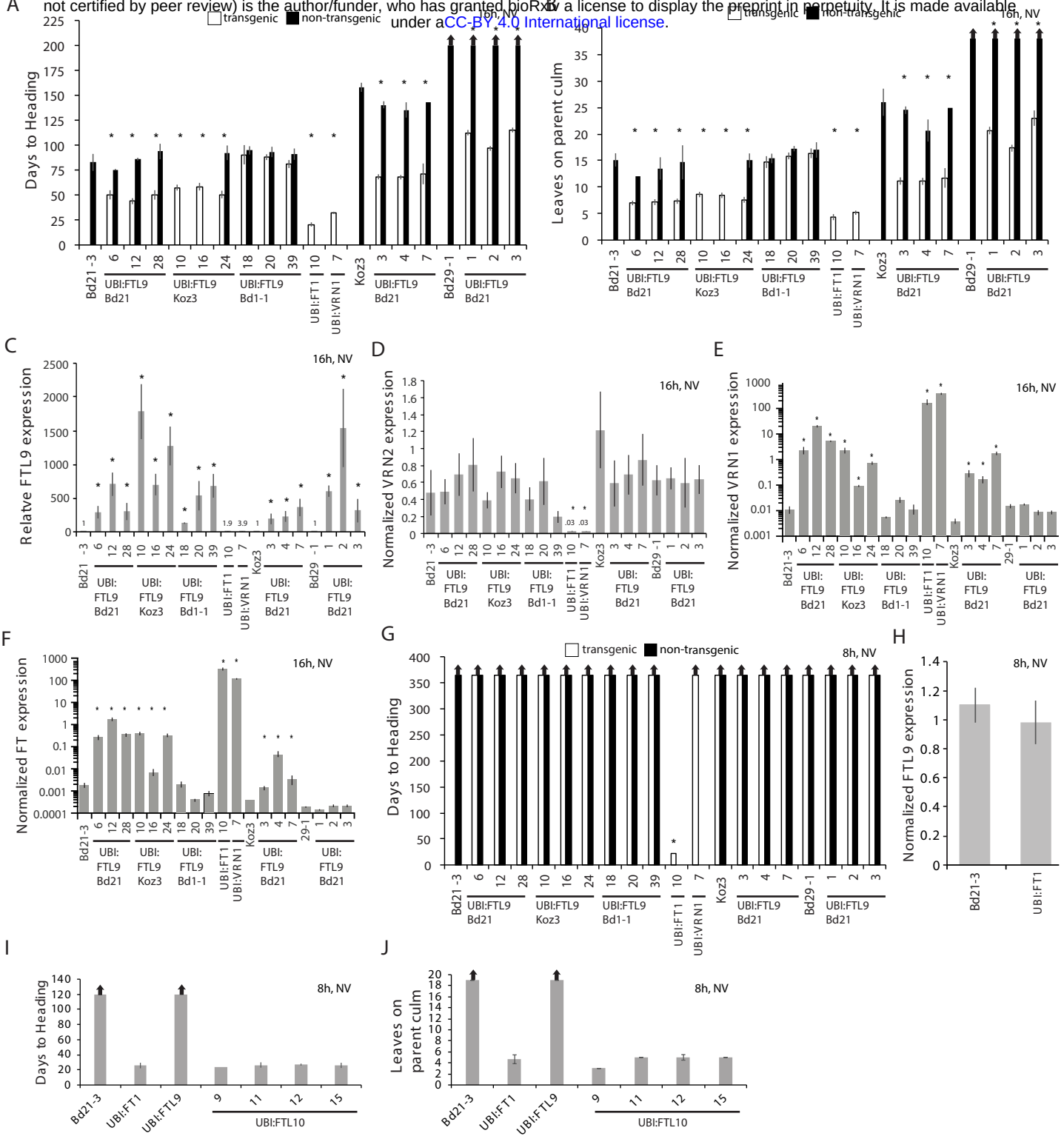

Figure 2-figure supplement 3. Effects of ubiquitin promoter-mediated constitutive expression of *FTL9*, *FTL10, FT1*, and *VRN1*
(**A-B**) Flowering times as days to heading (**A**) or final leaf count on parent culm at time of flowering (**B**) of independent *UBI:FTL9* transgenic lines (white bars) in Bd21-3, Koz3, and Bd29-1 compared with the respective wild-types and segregating non-transgenics (black bars). Lines with no non-transgenic plants are fixed for the transgene. Bars represent the average of at least 6 plants +/- SD. The experiment was repeated with similar results (data not shown). Arrows above bars indicate that none of the plants flowered at the end of the experiment. (**C-F**) Quantitative RT-PCR expression data from the upper leaf at the fifth leaf stage grown in a 16-h photoperiod. Expression data are normalized to *UBC18* and represent the average of three biological replicates +/- SD. Expression analyses were repeated with similar results. Single asterisks indicate P-values <0.01. NV, non-vernalized. *UBI:FT1* and *UBI:VRN1* transgenics are described in (Ream et al., 2014). *UBI:FTL9* Bd21 cDNA is from Bd21, *UBI:FTL9* Koz3 cDNA is from Koz3 and *UBI:FTL9* Bd1-1 cDNA is from Bd1-1. (**G**) Days to heading in 8h photoperiod non-vernalized (NV). Dissections on the parent culm revealed that the meristems were still vegetative after 150 days of growth in SD for all lines except *UBI:FT1* which flowers rapidly. (**H**) Quantitative RT-PCR expression data from the upper leaf at the third leaf stage grown in a 8-h photoperiod in *UBI:FT1* and Bd21-3. (**I**) Flowering times as days to heading (**J**) or final leaf count on parent culm at time of flowering of 4 independent *UBI:FTL10* T1 transgenic lines, *UBI:FT1* (T2 generation) and *UBI:FTL9* Koz3 line 10 from (**A**) in this figure (T1 generation).

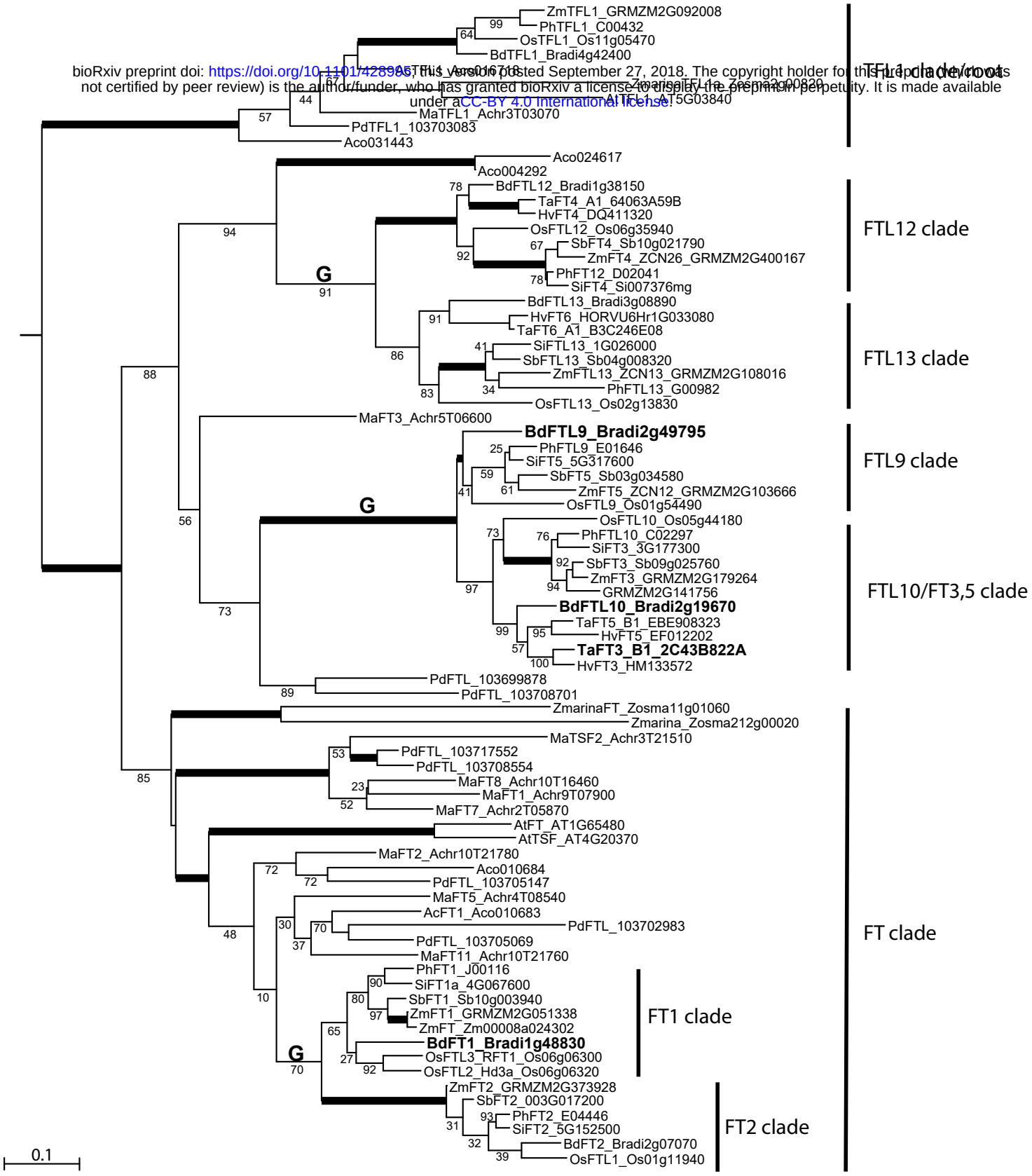

Figure 2- figure supplement 4. Maximum likelihood phylogenetic relationships among a subset of *FT*-like genes based on a nucleotide alignment of the PEBP domain. Maximum likelihood bootstrap support values indicated below branches with bold branches indicating bootstrap values of 100. “G” above branch indicates a grass-specific duplication. Scale bar indicates substitutions per site. Focal genes are labeled in large bold font. Note clades FTL9, 10, 12 and 13 contain only monocot species. Abbreviated species names: Bd, *Brachypodium distachyon*; Os, *Oryza sativa*; Ta, *Triticum aestivum*; Hv, *Hordeum vulgare*; Sb, *Sorghum bicolor*, Zm, *Zea mays*; Si, *Setaria italica*; Ph, *Panicum hallii*; Pd, *Phoenix dactylifera*; Ma, *Musa acuminata*; Z marina, *Zostera marina*; Ac, *Ananas comosus*; At, *Arabidopsis thaliana*. Sequence data was obtained from Phytozome v12 except sequence data for *P. dactylifera* was obtained from the KEGG database.

A

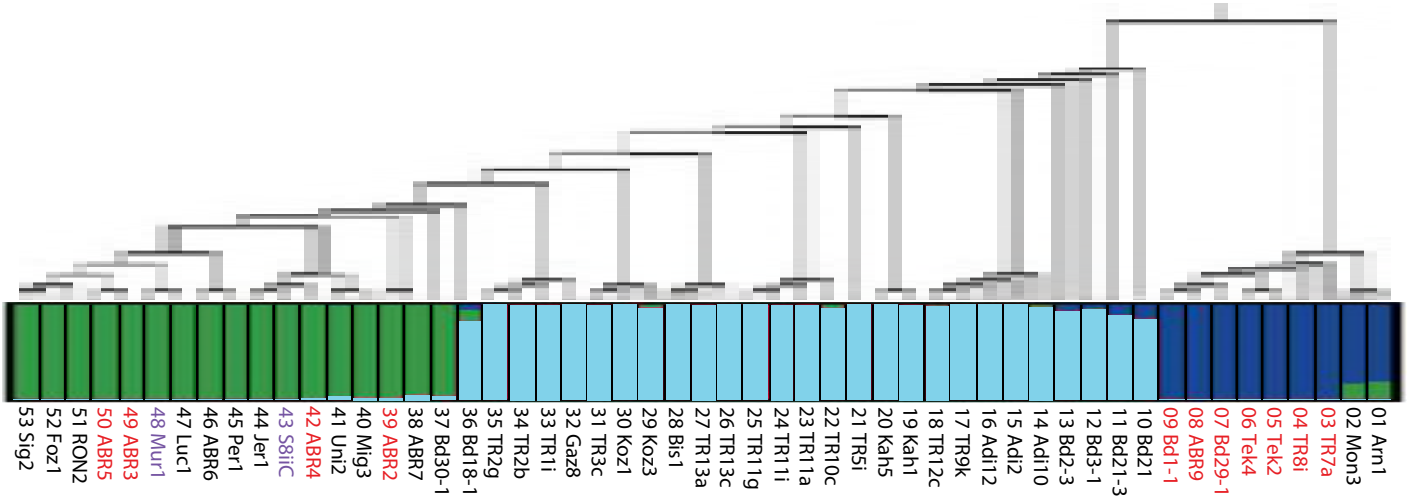

B

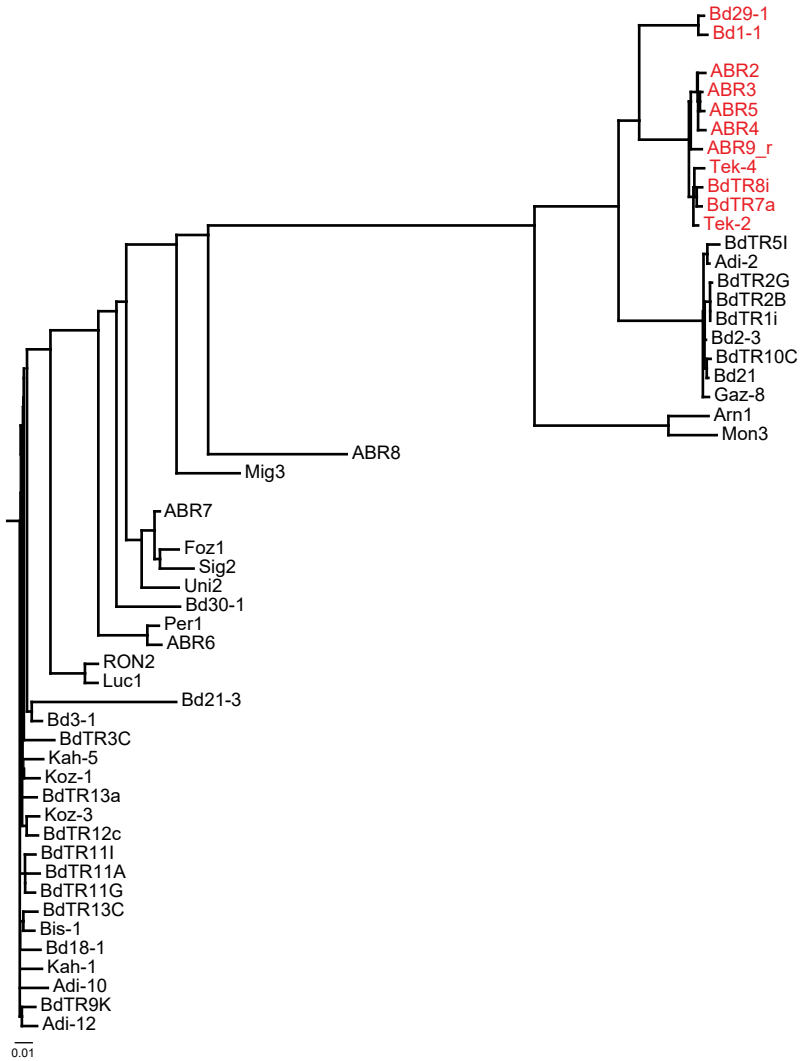

Figure 2-figure supplement 5 Population analysis (**A**) Maximum likelihood phylogenetic tree based on 3,933,264 SNPs spanning the genomes of 53 *B. distachyon* accessions, modified from (Gordon et al., 2017). Thickness of branches indicates bootstrap support: thick branches, 100%; intermediate, 70-99%; and thin, 50-69%. Red text indicates SD vernalization non-responsive accession, black text indicates SD vernalization responsive accessions, and purple text indicates accessions in which physiological experiments have not yet been conducted. Below the tree is a plot of individual membership (SNP profiles) to optimal K=3 Bayesian STRUCTURE groups: EDF+ miscellaneous (blue), middle eastern (light blue) and western european (green). (**B**) Phylogenetic analysis based on 940 SNPs spanning a 65kb mapped interval in which *FTL9* resides. Color of text same as (A). Scale bar indicates substitutions per site.

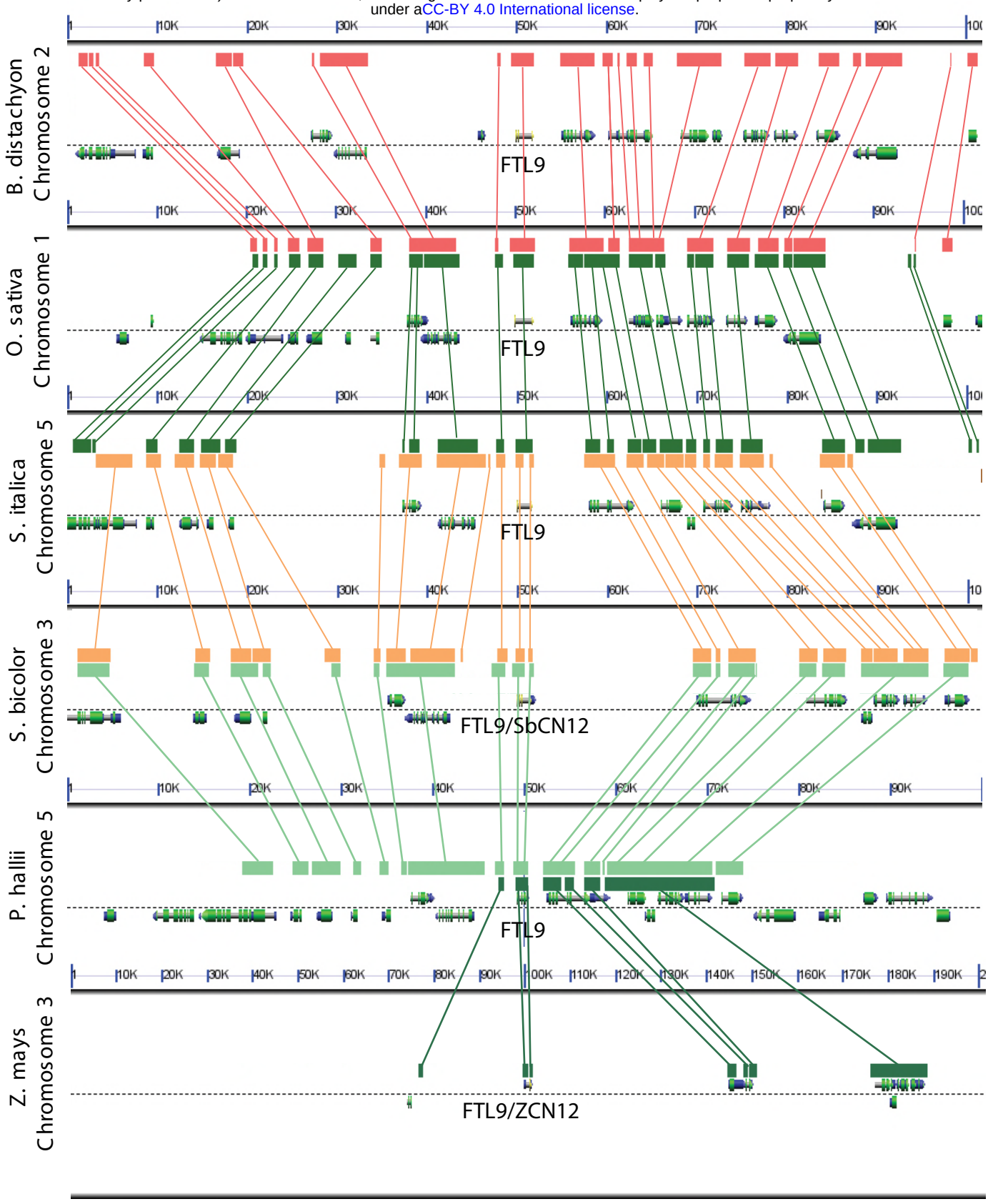

Figure 2-figure supplement 6. Analysis of syntenic chromosomal regions containing *FTL9* orthologs in grasses. Comparative analyses reveal conservation of gene order in an ~100kb genomic region around *FTL9* which supports the designations of *FTL9* orthologs throughout the grass family in the *FT*-like phylogenetic analysis in Figure 2-figure supplement 4 (Lyons et al., 2008).

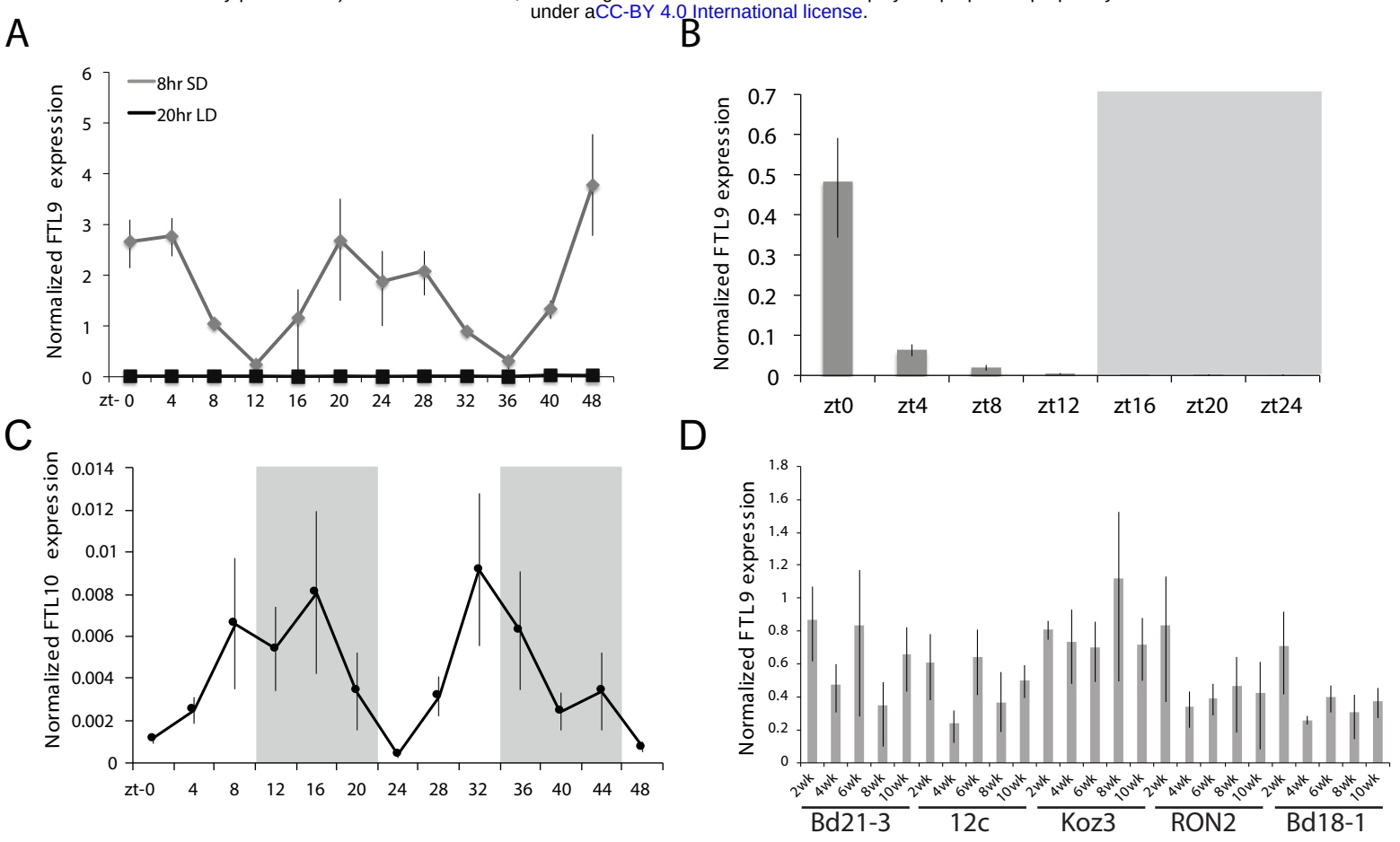

Figure 3-figure supplement 1. *FTL9* and *FTL10* diurnal mRNA expression. (**A**) Diurnal *FTL9* mRNA fluctuation in 8-h SD versus 20-h LD. Koz3 plants were grown in SD or LD until the fourth-leaf stage was reached at which point the newly expanded leaf was harvested at several time points throughout a 48-h diurnal cycle. In SD (8h light/16h dark) the dark periods were from zt 9-23 and 33-47. In LD (20h light/4h dark) the dark periods were from zt 20-23 and zt 44-47. (**B**) Plants were entrained under 8-h days until the fourth leaf stage was reached at which point the plant were grown in continuous darkness and the newly expanded fourth leaf was sampled every 4 hours for 24 hours. Shaded box represents subjective night. (**C**) Diurnal *FTL10* mRNA expression pattern in 8-h SD. For (**A-C**) values represent the average of four biological replicates +/- standard deviation (4 leaves per replicate). Shaded boxes represent dark periods. The experiment was repeated with similar results. Expression is normalized to *UBC18* as in (Ream et al., 2014). (**D**) *FTL9* mRNA expression in Bd21-3, 12c, Koz3, RON2 and Bd18-1 after 2-10 weeks of 8-h SD exposure. The newly expanded leaf on the parent culm was harvested at the end of the given SD treatment in the middle of the photoperiod. *FTL9* does not increase over time in SD in the accessions tested.

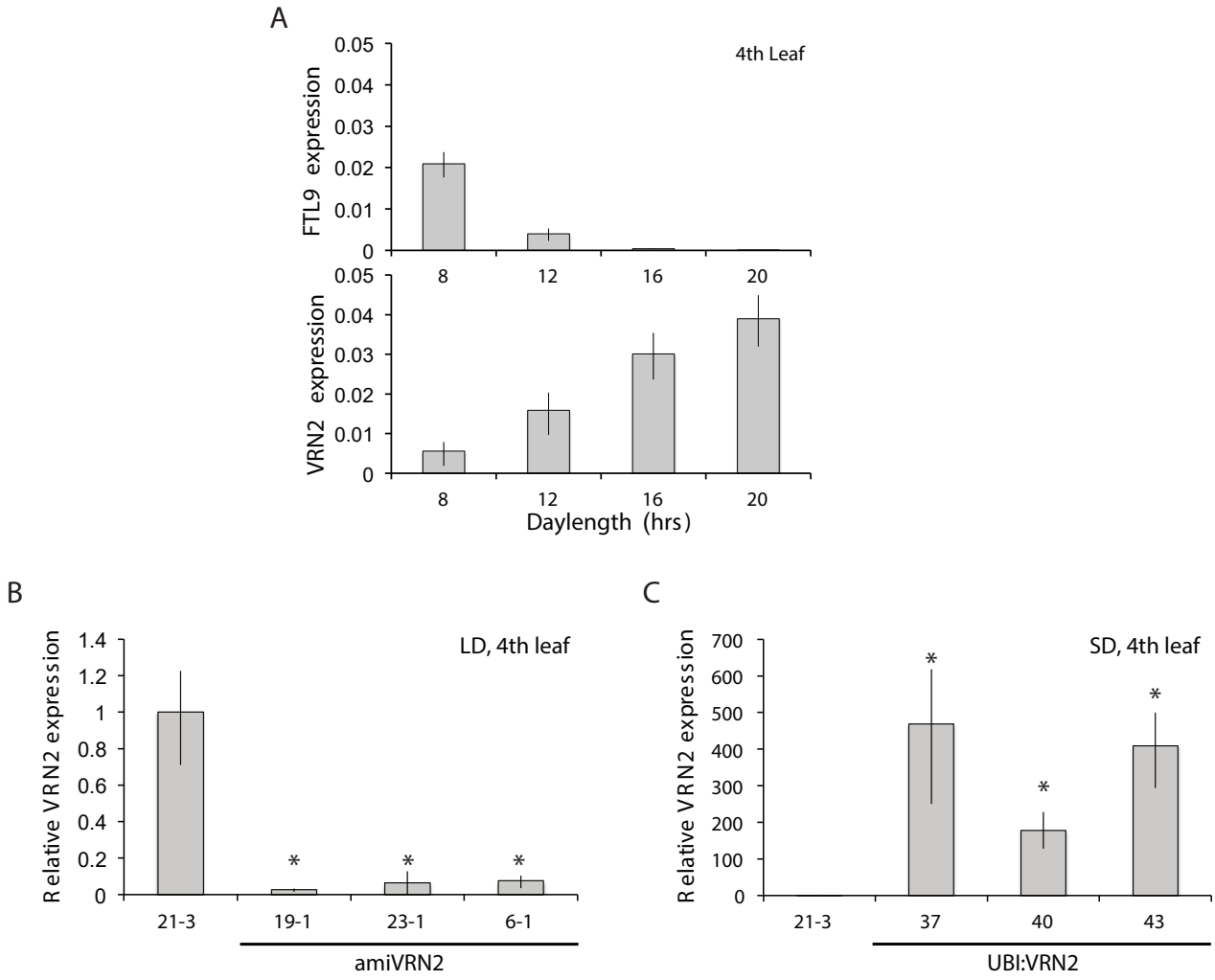

Figure 4-figure supplement 1. *FTL9* and *VRN2* expression in different photoperiods and in *amiVRN2* and *UBI:VRN2* transgenics. (**A**) *FTL9* (top) and *VRN2* (bottom) mRNA levels in 8, 12, 16 and 20-h photoperiods. Koz3 was grown to the fourth leaf stage and the newly expanded leaf was harvested in the middle of the photoperiod. (**B**) *VRN2* mRNA levels determined by quantitative RT-PCR from the upper leaf of Bd21-3 and *amiVRN2* plants at the fourth-leaf stage grown in a 16-h photoperiod (LD). (**C**) *VRN2* mRNA levels in the upper leaf of Bd21-3 and *UBI:VRN2* plants at the fourth-leaf stage grown in a 8-h photoperiod (SD). (A, B, C) Average relative *VRN2* expression is shown for four biological replicates +/- standard deviation (4 leaves per replicate). Asterisk indicate P-value <.05.